International Journal of Precision Engineering and Manufacturing-Green Technology
https://doi.org/10.1007/s40684-024-00621-z

Online ISSN 2198-0810
Print ISSN 2288-6206

REVIEW

Green Manufacturing of Electrically-Tunable Smart Light-Weight Planar Optics: A Review

Dongwook Yang[1] · Younggeun Lee[1] · Hyeokin Kang[2] · Quang Huy Vu[2] · Guseon Kang[1] · Seung Eon Lee[1] · Hyogeun Han[3] · Seunghwan Kim[3] · Han Ku Nam[1] · Soongeun Kwon[4] · Hyug-Gyo Rhee[5] · Joohyung Lee[2] · Hongki Yoo[1] · Hyosang Yoon[3] · Young-Jin Kim[1]

Received: 30 November 2023 / Revised: 11 March 2024 / Accepted: 13 March 2024
© The Author(s) 2024, corrected publication 2024

Abstract

Evolving demands for compact, light-weight, and versatile optical systems across various industries require the facile integration of planar diffractive optics. For the manufacturing of diffractive optics, green manufacturing becomes the prerequisite with timely considerations of Environmental, Social, and Governance (ESG). Conventional manufacturing processes such as semiconductor lithography or nano /micro imprinting utilize a large amount of harmful chemicals. Meanwhile, direct laser writing emerges as one of the key solution candidates, offering clear advantages over others, especially in terms of eco-friendliness due to the simple manufacturing process with less chemical usage. In this comprehensive review, we present recent advances in the analytical design, green manufacturing of electrically tunable smart light-weight planar optics, and their promising applications in space optics, photovoltaics, and optical imaging, highlighting the necessity for tunability in focal length, aberration, transparency, and beam propagation direction. Various types of electrically tunable diffractive optical elements utilizing active modulation of refractive index, geometrical shape, and bandgap have been discussed. Finally, this review concludes by proposing the integration of ultra-thin and light-weight diffractive optics presenting potential applications in micro-electronics, biomedical imaging, space exploration, and extended reality.

Keywords Green manufacturing · Diffractive optical element · Tunable planar optics · Laser direct writing

1 Introduction

1.1 Refractive, Reflective, and Diffractive Optics

Light can be manipulated via refractive, reflective, and diffractive optics. Refractive optics rely on the bending of light as it passes through materials with different refractive indices, such as lenses, to converge or diverge light rays. Reflective optics, on the other hand, employ mirrors to redirect light, maintaining its original wavelength and phase. Diffractive optics utilize the interference and diffraction of light waves, often through periodic structures, to shape and manipulate light, enabling devices like diffraction gratings and holograms [1–4]. Each of these optical approaches offers unique advantages and limitations, making them valuable tools in optical design, imaging, and various technological applications, depending on the specific requirements of a given system.

Diffractive optics exhibit several distinct advantages over refractive and reflective optics. One notable strength lies in

This paper is an invited paper (Invited Review)

✉ Young-Jin Kim
yj.kim@kaist.ac.kr

1 Department of Mechanical Engineering, Korea Advanced Institute of Science and Technology (KAIST), Daejeon 34141, South Korea

2 Department of Mechanical System Design Engineering, Seoul National University of Science and Technology (SEOULTECH), Seoul 01811, South Korea

3 Department of Aerospace Engineering, Korea Advanced Institute of Science and Technology (KAIST), Daejeon 34141, South Korea

4 Nano-Convergence Manufacturing Research Division, Korea Institute of Machinery & Materials (KIMM), Daejeon 34103, South Korea

5 Length and Dimensional Metrology Group, Korea Research Institute of Standards and Science (KRISS), Daejeon 305-340, Republic of Korea

their ability to achieve substantial reductions in thickness and weight. Diffractive elements can replace thick refractive lenses or bulky reflective mirrors with ultra-thin, lightweight surfaces that accomplish similar optical functions [2, 5, 6]. This characteristic is particularly advantageous in applications where space and weight constraints are critical, such as in aerospace and telecommunications systems. Furthermore, diffractive optics offer exceptional versatility in terms of optical design, enabling precise control of phase and amplitude, which is challenging to achieve with refractive or reflective components. This versatility makes diffractive optics well-suited for applications like beam shaping, spectral dispersion, and wavefront manipulation [7–9]. However, it's important to note that diffractive optics also have their limitations, including sensitivity to wavelength and limited efficiency, which must be carefully considered in their design and implementation.

Meanwhile, metasurfaces, which have recently attracted strong attention, also provide additional advantages over traditional optics, in terms of thickness, weight, and versatility. Unlike conventional optics, which rely on bulky and thick lenses or mirrors, metasurfaces are ultrathin, planar structures that manipulate light at the subwavelength scale. This property enables a dramatic reduction in thickness and weight, making metasurfaces highly desirable for applications where size and weight constraints are critical, such as in miniaturized optical systems and wearable devices [10–12]. Metasurfaces also provide precise control over the phase, amplitude, and polarization of light, allowing for the creation of complex optical functionalities in a single, compact layer. This versatility makes metasurfaces invaluable in areas such as beam steering, holography, and flat optics, offering a transformative approach to optical design and enabling the development of more compact, lightweight, and efficient optical systems [13–15]. However, it's important to note that metasurfaces are still subject to challenges, including limitations in the operating wavelength range and fabrication complexities that must be addressed for widespread adoption in practical applications.

1.2 Green Manufacturing Process for ESG

In the realm of semiconductor manufacturing, planar optical elements, and flat diffractive optical elements (DOEs) undergo fabrication through a series of semiconductor processes or traditional cutting methods. The production of thin, flat DOEs within the semiconductor industry involves a multi-step process that significantly impacts Environmental, Social, and Governance (ESG) considerations and green manufacturing practices.

Typically, in the case of DOEs, intricate patterns ranging from hundreds to several nanometers in size are meticulously created through a repetitive lithography process. Materials such as silicon and gallium arsenide, commonly used in semiconductor processes, are employed, with a substantial amount of energy consumed during the production of these ingots. The conventional Czochralski growth process historically consumed up to 100 kW/h per kilogram of silicon ingot produced [16]. However, advancements in modern furnace designs, continuous silicon feedstock supply methods, and improvements in gas flow dynamics have significantly reduced this energy consumption to less than 40 kW/h [16, 17]. Despite these improvements, addressing ESG policies remains crucial, particularly as the energy used in silicon ingot production often relies on fossil fuels. Continuous technological developments are essential to further minimize energy consumption and align with sustainable practices.

The semiconductor manufacturing process demands meticulous and sophisticated waste treatment and management practices to mitigate the ecological footprint associated with compounds such as photoresist, polishing slurry, and various etching materials. A prominent South Korean chip manufacturing company engaged in mass production utilizes over 150 chemical components across more than 450 chemical products, resulting in an annual consumption of over 45,000 tons of chemicals [18, 19].

An alternative method for fabricating flat optical elements is through traditional subtractive manufacturing. However, this approach generates various gases, chemical additives, coolants, lubricants, fuel energy, and cutting residues during processing. For instance, chlorine-based, fluorine-based, and boric acid-based vapors emitted during glass manufacturing, along with substances like sodium nitrate, potassium nitrate, and sulfate used as oxidizing and reducing agents to control glass properties, are considered hazardous substances or carcinogens [20].

This traditional manufacturing practice contributes to significant environmental damage through the release of hazardous waste and emissions. Coolants and lubricants introduce pollutants that can contaminate water sources, while factory emissions contribute to air pollution. The high power and energy demand also lead to increased carbon emissions, exacerbating climate change. Failing to address these challenges in traditional manufacturing hinders the industry's environmental stewardship [21].

Green manufacturing practices, involving the reduction of hazardous substances, optimization of energy usage, and the adoption of sustainable materials and recycling, become essential to align these technologies with ESG goals. By addressing the environmental impact associated with these processes, industries can demonstrate their commitment to responsible ESG practices and contribute to a more environmentally conscious and sustainable future. In the context of ESG considerations, the practices in traditional semiconductor and machining processes often conflict with environmental responsibility. To align with ESG principles and embrace green manufacturing, a transition to sustainable machining technologies and processes is imperative. This shift minimizes resource consumption, reduces waste generation, and prioritizes energy efficiency in the manufacturing of ultra-thin smart optics. Through such efforts, industries can mitigate their environmental footprint, adhere to ESG commitments, and contribute to a more environmentally sustainable manufacturing landscape.

1.3 Light-Weight Planar Optics: Key Requirements

Planar optics for photovoltaics, smart windows, and smart lighting are highly required, as described in Fig. 1. Light-weight deployable planar lenses represent a promising technological innovation for space satellite applications. These planar lenses, which can be compactly stowed during launch and then unfurled or deployed in space, offer several advantages. They enable the miniaturization of satellite payloads, reducing launch costs and providing increased mission flexibility. Deployable planar lenses can be used for a variety of purposes, such as enhancing imaging capabilities, enabling compact radar systems, or improving communication systems by focusing and steering electromagnetic waves. Their planar and lightweight design makes them well-suited for integration into small satellites or CubeSats. The deployment mechanism, materials, and precise control systems are key considerations in designing these lenses for space deployment. As technology advances and deployment mechanisms become more reliable, deployable planar lenses are likely to find increasing utility in future space missions, contributing to more cost-effective and versatile satellite systems. Light-weight mobile camera lenses are of paramount importance in modern high-performance mobile phone cameras, offering portability and versatility in capturing high-quality images and videos. Their manufacturing

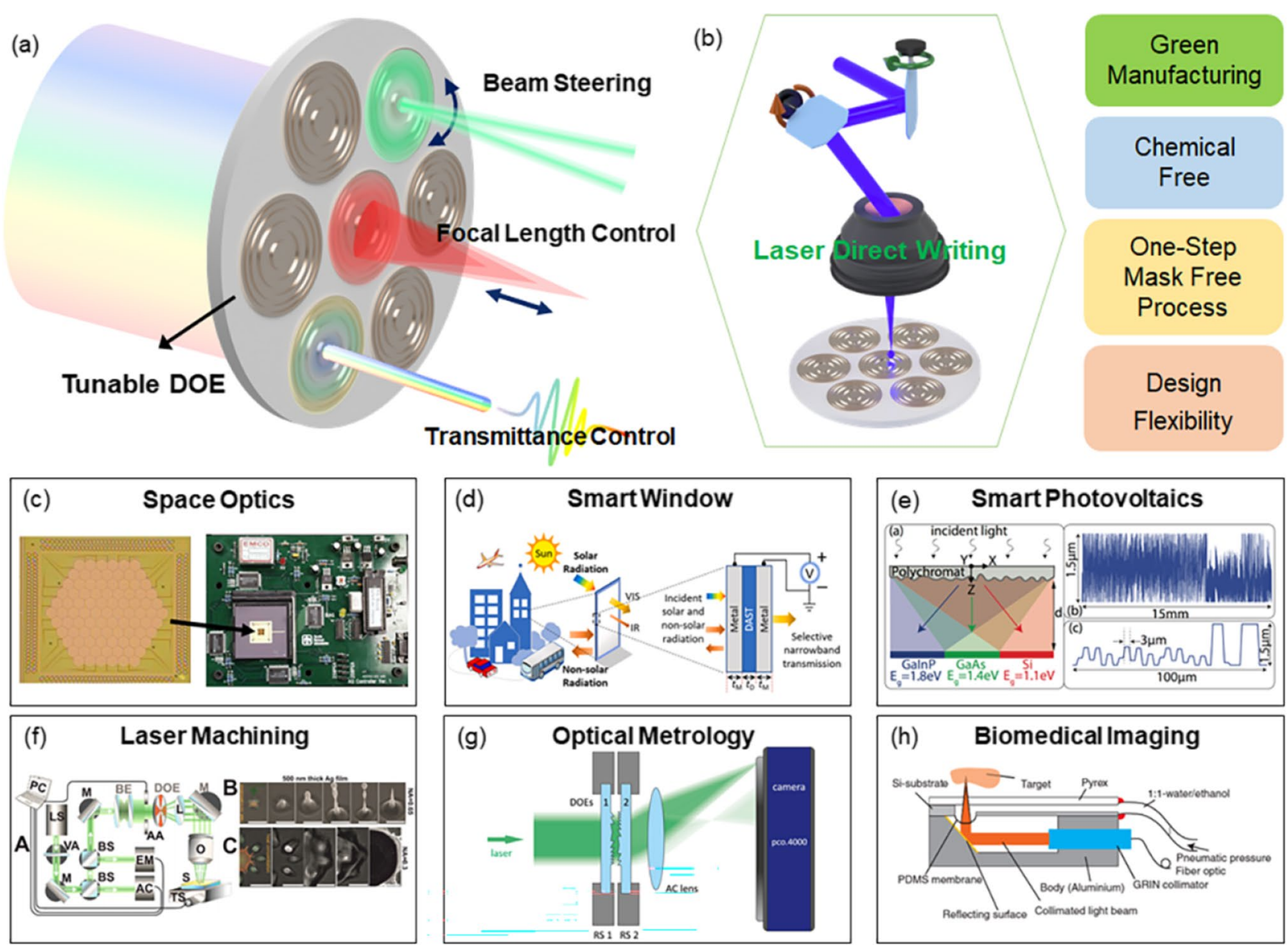

Fig. 1 **A**) Tunability requirements of tunable DOE including beam steering, focal length control, and transmittance control (**b**) Advantages of laser direct writing (c-h) Applications of tunable DOE. (**c**) Space optics (Adopted from [22] Figure 1) (d) Smart window (Adopted from [23], Figure 1) (e) Smart photovoltaics (Adopted from [24], Figure 1) (f) Laser machining (Adopted from [25], Figure 3) (g) optical metrology (Adopted from [26], Figure 3) (h) Bio application (Adopted from [27], Figure 12)

methods often involve the use of advanced materials like plastic and composite elements to reduce weight while maintaining optical performance. The advantages of lightweight mobile camera lenses include improved ease of use, reduced strain on device components, and enhanced image stabilization. These lenses also contribute to the overall reduction in device weight and size, making them indispensable for mobile devices where portability and user experience are critical. Research efforts are continually focused on developing novel materials, optical designs, and fabrication techniques to further enhance lightweight lens performance, ensuring that mobile cameras continue to meet the demands of today's tech-savvy consumers. Thin endoscopic probes hold importance for minimally invasive procedures and diagnostics in medical applications. Their manufacturing typically involves the use of advanced materials and precision machining techniques to create compact, lightweight, and flexible optical systems that can navigate the narrow and tortuous pathways of the human body. The advantages of thin endoscopic probe optics include reduced patient discomfort, shorter recovery times, and fewer complications compared to traditional open surgeries. Moreover, their small size and flexibility allow access to previously inaccessible regions within the body, facilitating precise imaging, diagnostics, and therapeutic interventions. Ongoing research focuses on further miniaturization, enhanced imaging capabilities, and integration with other diagnostic and therapeutic tools, ensuring that thin endoscopic probe optics continue to advance medical practices and improve patient outcomes.

1.4 Tunable Planar Optics: Key Requirements

The smart tunability of ultra-thin optics is crucial for their adaptability and versatility in a variety of optical applications stated above. Key requirements for tunability include the ability to adjust focal length, enabling precise focusing and imaging; the control of aberrations, minimizing optical distortions for high-quality imaging; transparency modulation, allowing for dynamic light transmission adjustments; and the capability to manipulate beam propagation angles, facilitating beam steering and redirection [28–32]. Achieving these tunability requirements typically involves the integration of advanced materials, such as liquid crystal or electroactive polymers, and the incorporation of responsive mechanisms, like piezoelectric actuators or voltage-driven devices [33–36]. Meeting these requirements empowers ultra-thin optics to address a broad range of optical design challenges and adapt to dynamic operating conditions, making them valuable tools in contemporary optical systems.

2 Design and Fabrication of Diffractive Optical Elements

2.1 Design of Diffractive Optical Elements

The design of DOEs conventionally has been pursued through an analytic solution-based approach derived from the Rayleigh-Sommerfeld diffraction integral [37–40]. While this theory offers intuitive solutions for straightforward imaging function of the diffractive optics, recent demands for various functionalities in DOEs, and the requirements for a rapid design process have led to the adoption of numerical optimization-based approaches to overcome the limitations of the conventional analytic solution-based approaches [41–43]. The numerical design approach already has been successfully applied to various DOEs implementations, such as achromatic imaging DOE, multiple elements DOEs, large-scale optics, hybrid optics, and photon sieves [44–52].

The numerical design process for DOEs consists of three representative steps, including phase optimization, pattern generation, and verification, which can be further divided into detailed procedures, as shown in Fig. 2(a). The phase optimization step involves optimizing phase parameters to minimize or maximize merit functions, aiming to achieve the optical specifications of the target DOE. As shown in Fig. 2(a) (step 1), a continuous phase map across the entrance pupil can be generated by using polynomials with the function of spatial variables in commercial ray-tracing tools. For the modeling of symmetric or asymmetric surface phase, Zemax® provides the surface types of "binary1" and "binary2", respectively [53]. These surface types comprise various orders of polynomials with coefficients, which can be optimized to minimize merit functions. Subsequently, the optimized phase map is applied to a modulo operation concerning 2π, resulting in a residual map that corresponds to the kinoform profile, as shown in Fig. 2(a) (step 2). The extracted phase map of the kinoform is then quantized, as shown in Fig. 2(a) (step 3), during the DOE pattern generation process. Depending on the efficiency requirements and fabrication feasibility, threshold values can be set to create either single-level or multiple-level patterns. Increasing the number of levels can enhance efficiency from 10 to 99% [35]. This pattern generation and quantization process allows rapid calculations by importing the optimized phase map data from the ray-tracing software into computation software such as MATLAB® or Python®. The performance of the generated DOE pattern can be verified using physical optics propagation (POP) within ZEMAX®, which is based on scalar diffraction theory. The POP function allows the evaluation of primary optical specifications, such as focal

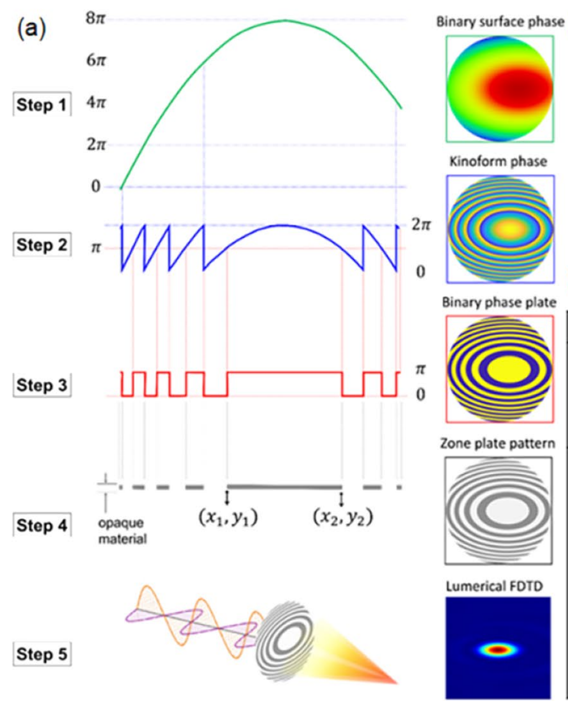

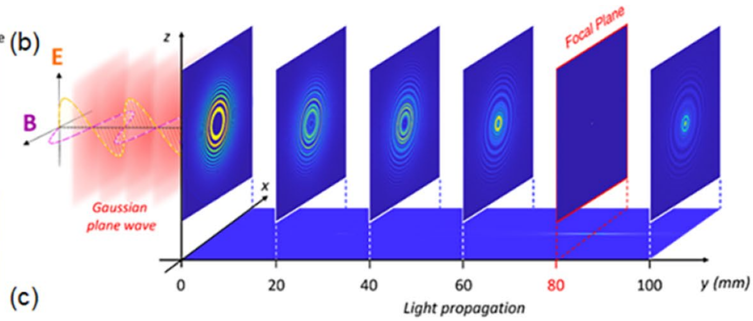

(c)

	Structure	Name	Efficiency
Refractive optics		Commercial lens (Bulk lens)	100%
		Fresnel lens (not THz range Radiation) (From Surface Sag)	100%
Diffractive Optics		Fresnel zone plate (Amplitude binary)	10.1%
		Planar dielectric zone plate (Structure created from 2 materials)	10.1%
		Binary Fresnel Phase Plate (Phase-reversing or Level-2 zone plate)	40.4%
		Multi-level Zone plate (Level-4, Level-8 ... plate)	81% - 99%
		Kino-form, Fresnel diffractive lens (From Surface phase)	100%

Fig. 2 **A** Design process of DOEs. The comprehensive DOE design process consists of 5 steps, incorporating optimization of the surface phase, conversion to Kinoform/binary phase, and verification of the pattern. Each step utilizes ray-tracing, computational, or finite element analysis software as appropriate for precise modeling and optimization. (**b**) Verification of a diffractive pattern in the design process. The designed pattern can be imported for the verification of beam propagation characteristics, including amplitude, phase, and wavefront, in both near-field and far-field regions by using ray-tracing or finite analysis tools. (**c**) Analytical design and efficiency of refractive optics and diffractive optics (adopted from [35] Table 1)

length, f-number, spot size, and depth of focus. Figure 2(b) presents the results of imported a 1-inch diameter DOE pattern with focal length 80 mm, estimating beam profiles depending on propagation distance. In the near-field, the DOE pattern transfers directly to the beam profile, however as the beam propagates, the beam size gradually shrinks, focusing a spot accurately at the 80 mm focal length. Beam cross-sections are plotted against propagation distance, allowing depth of focus evaluation at the focal length. Additionally, it clearly reveals side-effects such as focusing due to high-order diffraction in the near-field. For cross-evaluation purposes, Finite-Difference Time-Domain (FDTD) software also enables the verification of the DOE pattern, as shown in Fig. 2(a) (step 5) [54, 55]. Additionally, evaluation in the FDTD with a more versatile configuration is available, such as DOE illumination with oblique incident angles or sources with divergence angles, which is not fully supported in the ray-tracing software [53]. Once the design and verification processes are completed, the pattern is prepared for fabrication through drawing work. The resolution of drawing files, such as gds or dwg, is adjusted with accounting for fabrication precision, and efficiency of the drawing work flow.

Diffractive optics employ micro- or nanostructures etched onto a flat surface to control the phase and amplitude of incident light waves. This precise control over light wavefronts enables ultrathin, planar optical elements capable of achieving complex optical functions. Diffractive optics offer several advantages over traditional refractive optics, including reduced thickness and weight, as well as the ability to correct chromatic aberrations and implement multifunctional optical elements. These characteristics make diffractive optics particularly valuable in applications where space and weight constraints are critical, such as in compact imaging systems and wearable devices, offering a versatile and lightweight alternative to traditional refractive optics. Ultrathin diffractive optics design encompasses various techniques, including the use of Fresnel zone plates, binary Fresnel phase plates, and kinoforms, which differ significantly from traditional optics design. Fresnel zone plates use concentric rings with varying widths to focus light, while binary Fresnel phase plates employ discrete phase levels to manipulate wavefronts, enabling lightweight and compact optical elements. Kinoforms, on the other hand, optimize the phase distribution to achieve specific optical functions, minimizing energy loss. These ultrathin designs offer advantages like reduced thickness, weight, and chromatic aberrations compared to traditional bulky lenses or mirrors. Thus, they are well-suited for applications where size and weight constraints are paramount, such as in portable imaging devices, augmented reality displays, and miniaturized optical systems, representing a transformative approach to optical design and enabling more compact and lightweight optical solutions.

2.2 Traditional Manufacturing Methods for DOE

The manufacturing process of thin, flat diffractive optical elements (DOEs) in the semiconductor industry involves numerous steps that impact ESG considerations and green manufacturing practices. Typically, in the case of DOEs, aligned patterns ranging from hundreds to several nanometers in size are created through a repetitive lithography process. The materials used in DOEs, such as silicon or gallium arsenide, are common in semiconductor processes, and the production of these ingots consumes vast amounts of energy. Additionally, the vacuum environment in which general photolithography processes occur increases energy consumption in the overall process [56–59].

A variety of compounds are employed in actual semiconductor manufacturing. Due to security considerations in the semiconductor industry, determining the exact composition of materials is often challenging [60–63]. Nevertheless, a range of substances, including resin, photoresist (PR), polymer compounds, surfactants, organic acids, organic compounds, pigments, and more, are commonly utilized. The manufacturing process incorporates a minimum of five substances, including sulfuric acid, chromic acid, ethylene oxide, silica, potassium dichromate, etc., all of which fall under Group 1 carcinogens as per the classification by the International Agency for Research on Cancer (IARC) [64–68]. Additionally, the process may involve the use of Group 2B carcinogens, including diborane, carbon black, 1,4-dioxane, pyrocatechol, antimony trioxide, methyl isobutyl ketone, ethylbenzene, diethanolamine, titanium dioxide, lead, dichloromethane, naphthalene, alpha-methyl, styrene, 1,2-benzenediol, nitrilotriacetic acid, cumene, among others [18, 69, 70].

Furthermore, the semiconductor process utilizes substances such as ethylene oxide and hydroquinone, as well as phenol and N-butyl glycidyl ether, all categorized as Group 2 germ cell mutagens and falling under Group 1B. Reproductive toxicants in the semiconductor process are categorized into different groups. Group 1A includes carbon monoxide and lead, whereas Group 1B encompasses 2-ethoxyethanol, 2-methoxyethanol, ethyl cellosolve acetate, N, N-dimethylacetamide, and sodium tetraborate. Additionally, Group 2 reproductive toxicants consist of toluene, cyclohexylamine, and hexane [18].

Addressing ESG concerns and advancing green manufacturing in this context involves exploring alternative materials and more environmentally friendly processes [71, 72]. This includes investigating sustainable substrates and coatings, as well as developing energy-efficient etching techniques, such as plasma etching [73]. Additionally, waste reduction and recycling efforts can be implemented, and the adoption of green energy sources for manufacturing facilities can minimize the carbon footprint associated with the energy-intensive aspects of the process [57]. Furthermore, research into the integration of cleaner and more sustainable fabrication methods, such as nanoimprint lithography, holds potential for reducing the environmental impact of thin, flat DOE production. By taking these steps and embracing green manufacturing principles, the semiconductor industry can work towards more eco-friendly and sustainable production of DOEs, aligning with global efforts to reduce the environmental impact of technology manufacturing.

2.3 Direct Laser Writing

Direct Laser Writing (DLW) has emerged as a forefront manufacturing technique, presenting several key advantages over precedent methods [74–78]. One of its most noteworthy attributes is its green manufacturing profile due to the facile process and wide selection of materials [79–82]. DLW significantly reduces the environmental impact compared to methods like photolithography, primarily due to its elimination of hazardous chemicals [83–85]. Unlike photolithography, which relies on photoresists, developers, and etching chemicals, DLW is a direct-write process that operates without the need for such environmentally harmful materials. It offers a wide range of substrate options including glass, textiles, and biomass materials such as wood, leaves, and charcoal [5, 86, 87]. By virtue of its chemical-free approach, DLW not only reduces waste generation but also minimizes the risk of environmental contamination [88–91].

Additionally, DLW systems can be more energy-efficient, working with simple manufacturing processes without the need for specialized treatments. The facile processing steps and the direct utilization of energy from the laser source contribute to its energy efficiency [92–97]. Moreover, DLW systems can often be operated with lower power requirements, further reducing their environmental footprint [98, 99]. In terms of future developments, ongoing research in DLW technology aims to enhance its green manufacturing techniques. This includes exploring new materials that are more environmentally friendly, optimizing process parameters to minimize energy consumption, and integrating DLW with other sustainable manufacturing processes. Collaborative efforts between researchers and industry partners are driving innovations in DLW technology, guiding the way for even greener and more eco-conscious manufacturing processes in the future.

2.4 Nanoimprinting

Nanoimprinting is a nanofabrication technique based on the principle of replicating nanoscale patterns from a master template onto a substrate. It involves pressing the template, containing desired nanostructures, into a soft, moldable material that solidifies upon cooling or exposure to UV light, resulting in precise replication of nanostructures on the substrate's surface [100–105]. Nanoimprinting offers a greener and more eco-friendly alternative to traditional semiconductor lithography [106–110]. Unlike conventional lithography, which often uses hazardous chemicals and energy-intensive processes, nanoimprinting generally requires fewer chemicals, emits fewer volatile organic compounds, and consumes less energy [111–113].

Additionally, the process can utilize biodegradable or recyclable materials, further reducing its environmental impact [102]. This enhanced eco-friendliness and reduced power consumption make nanoimprinting a promising and sustainable choice for nanofabrication, aligning with green manufacturing practices and contributing to a more energy-efficient and environmentally conscious technological landscape [114–117]. Looking ahead, advancements in nanoimprinting technology hold promise for even greater sustainability gains. Continued research efforts are focused on improving process efficiency, exploring novel materials with enhanced eco-friendliness, and addressing any remaining challenges in scalability and cost-effectiveness [118]. By addressing these aspects, nanoimprinting can further solidify its position as a key enabler of green manufacturing practices, contributing to a more sustainable technological landscape.

3 Electrically-Tunable Planar Optics

Figures 3, 4, 5, 6, 7, 8, 9 illustrates the principle of tunable DOE with optical tuning effect, medium, and the principle of operation. Optical tuning can be realized by active modulation of refractive index with liquid crystals, active modulation of geometry of fluid and elastomer, and active modulation of the bandgap of 2D materials. We have discussed these cases one-by-one in detail in this forthcoming section.

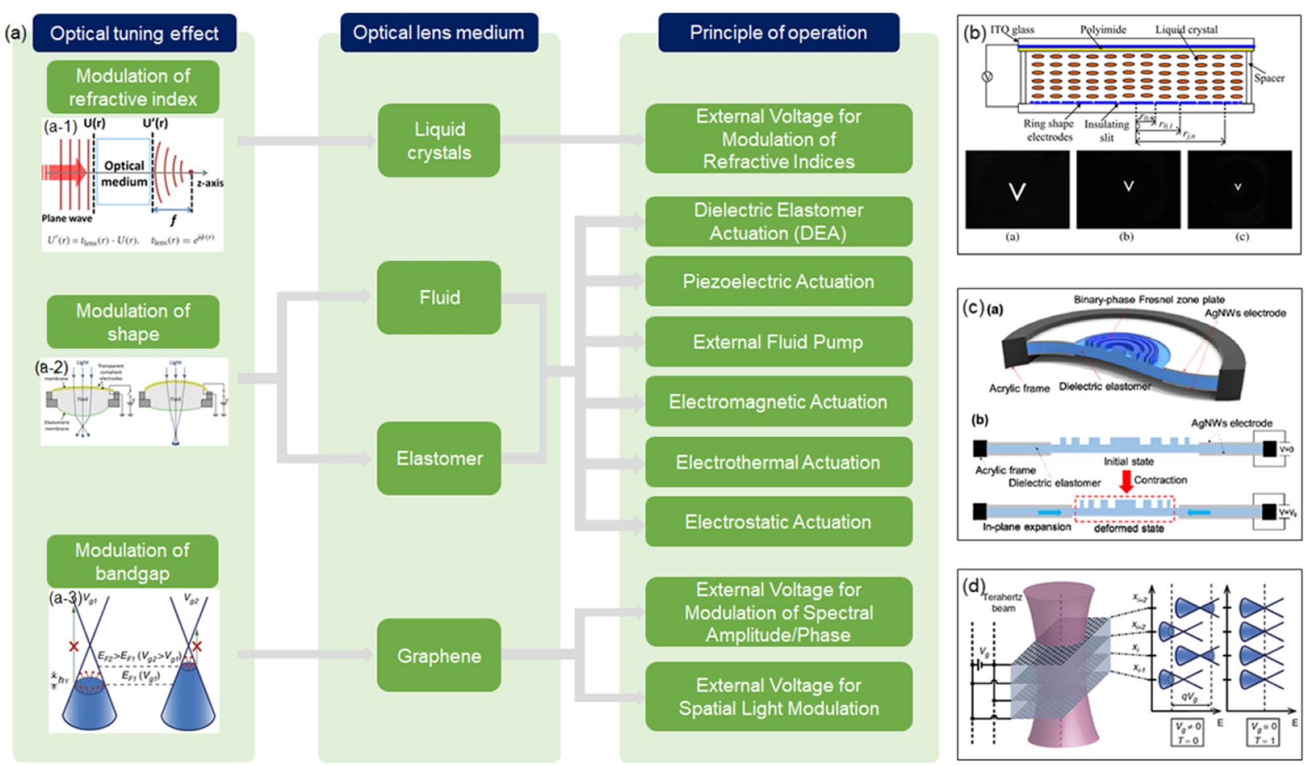

Fig. 3 Principle of tunable DOE: (**a**) Optical tuning effect, lens medium, and the principle of tunable DOE (a-1) Principle of liquid crystal (adopted from [119] Figure 1) (a-2) Principle of modulation of shape (adopted from [36] Figure 4) (a-3) Principle of modulation of bandgap (adopted from [120] Figure 1) (**b**) Tunable DOE enabled by liquid crystal (adopted from [121] Figure 2) (**c**) Tunable Fresnel zone plate enabled by modulation of shape (adopted from [122] Figure 2) (**d**) Modulation of bandgap of terahertz beam (adopted from [120] Figure 1)

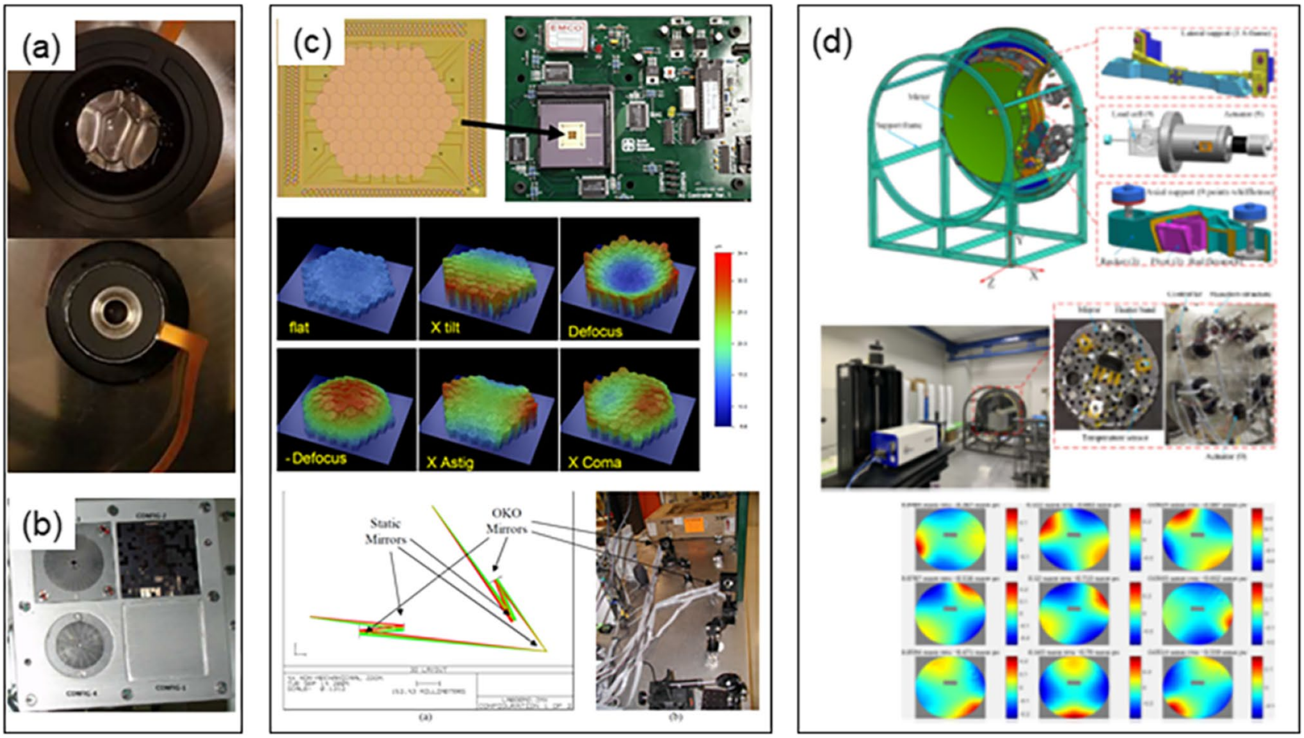

Fig. 4 (**a**) Corning's electrowetting-based liquid lens in a soft vacuum setting and Optotune's pressure-driven liquid lens in a soft vacuum setting (Adopted from [123], Figure 4 and 6) (**b**) 91 element hexagonal piston-tip-tilt mirror array with a ~ 4 mm active aperture packaged on controller board. Zernike aberrations were created with an array of 61 piston-tip-tilt micromirrors with 27-μm stroke. ZEMAX® and experimental layouts of the 4X active optical zoom (Adopted from [124], Figure 1, 2, and 10) (**c**) 0.676 m SiC lightweight mirror assembly showing the support frame, mirror body, passive support, and active support. For clarity, part of the model has been cut off along the wave lines. Integrated system on its test platform showing the experimental apparatus of heat and active optics. Influence functions of mirror surface in which the piston and tilt have been removed, measured with a Fizeau interferometer. (Adopted from [22], Figure 1, 6, and 9) (**d**) Four different configurations of shadow-casters and detectors were leveraged in the payload. CONFIG-3 and CONFIG-4 contained Fresnel zone plates as shadow-casters (Adopted from [125], Figure 2)

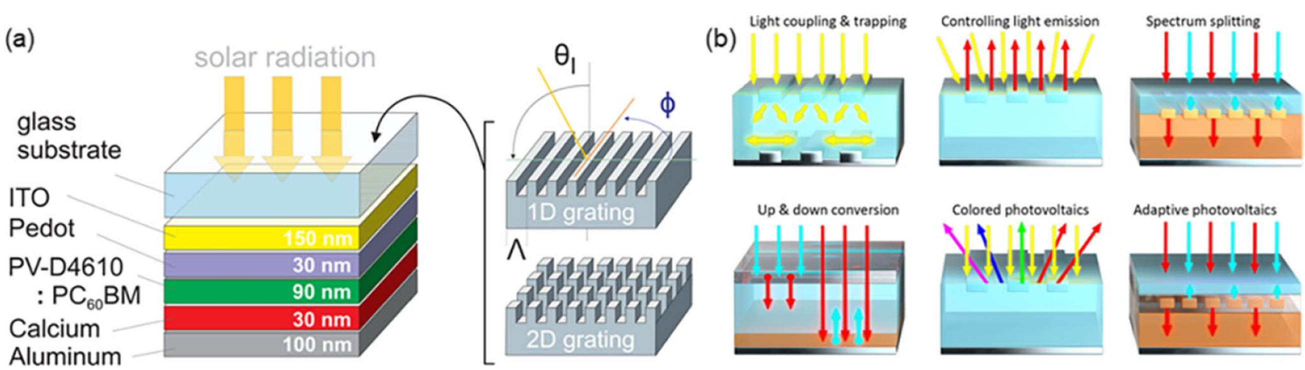

Fig. 5 Smart photovoltaic applications (**a**) enhanced light-harvesting in photovoltaic devices enabled by gratings (Adopted from [126], Figure 1) (b) light management to optimize the photovoltaics (Adopted from [127], Figure 2)

3.1 Active Modulation of Refractive Index

The modulation of refractive index by liquid crystal (LC) materials is a pivotal technique for achieving electrically tunable Diffractive Optical Elements (DOEs) with versatile optical functionalities. LCs often exhibit anisotropic optical properties due to their orientation-dependent refractive indices. The principle lies in the ability of LC molecules to align themselves under the influence of an external electric field, thereby changing the refractive index experienced by incident light [134–136, 137]. By patterning the alignment of LC molecules on substrates and applying an electric field,

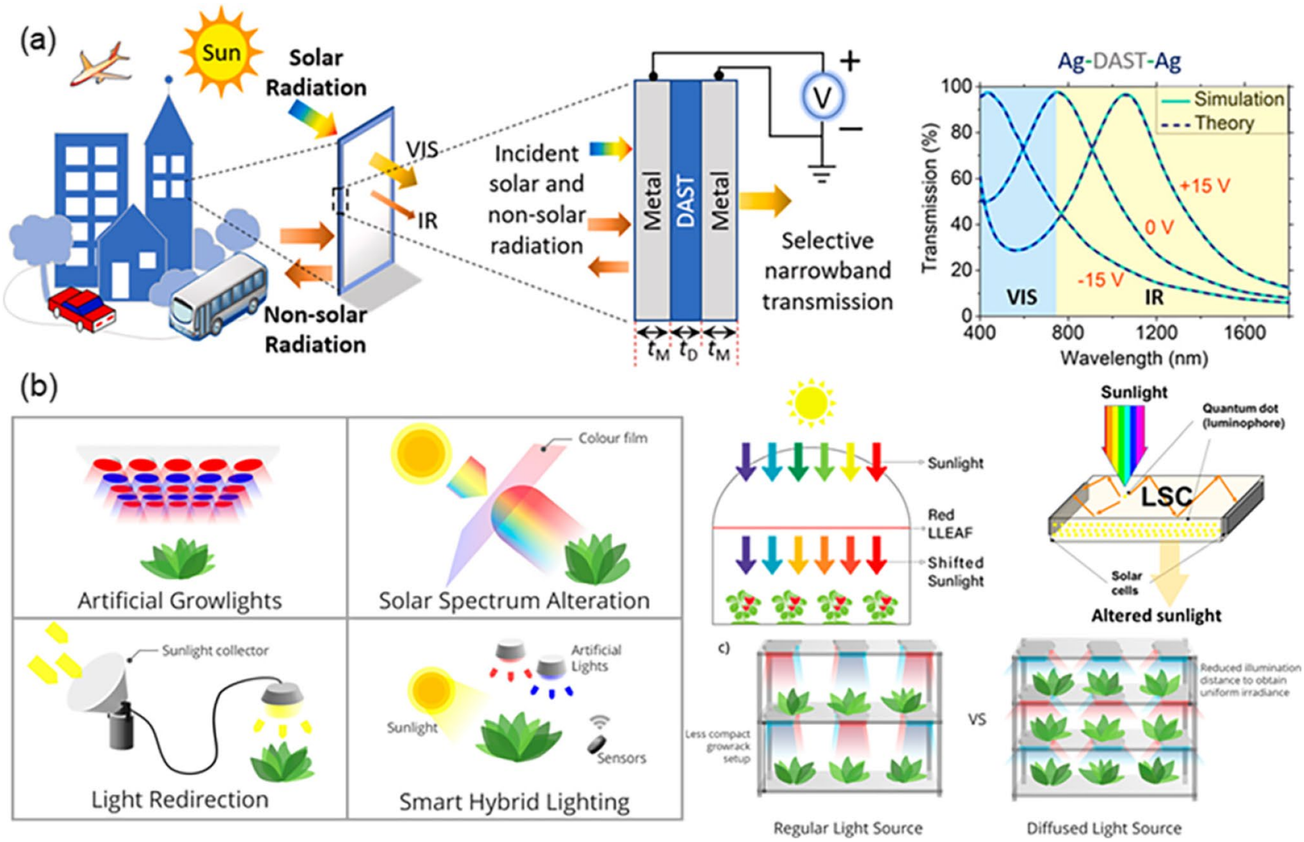

Fig. 6 Smart window and light (**a**) Solar radiation transmittance control for effective heating (Adopted from [128], Figure 1) (b) Effective light management for harvesting enabled by transmittance and diffusion control (Adopted from [129], Figure 5 and 6)

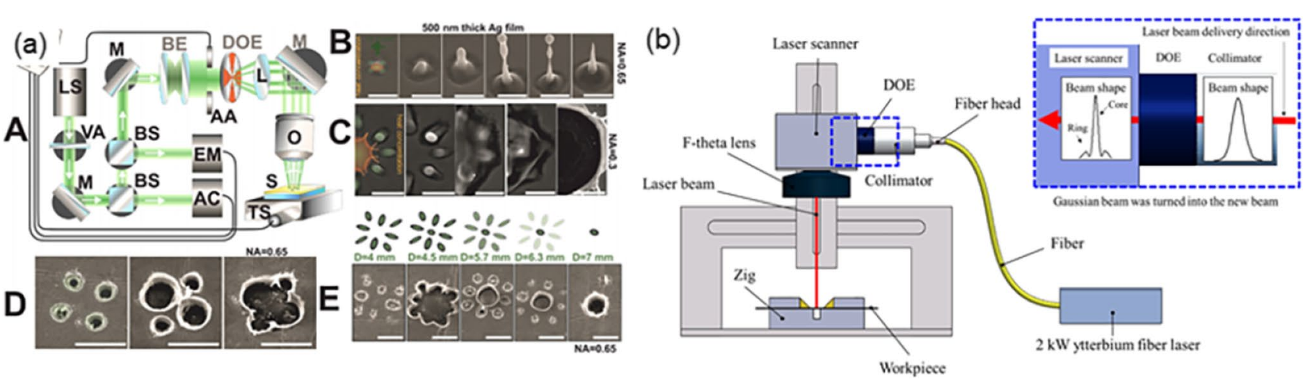

Fig. 7 DOE applications for laser machining (**a**) Beam splitting enabled by DOE for effective nanofabrication of Ag film (Adopted from [25], Figure 3) (b) Beam shaping accomplished by DOE for effective laser welding of aluminum alloy (Adopted from [130], Figure 1)

precise control over the phase and amplitude of light passing through the LC layer can be achieved. This dynamic modulation enables the creation of electrically tunable DOEs [138–141]. The applications of LC-based DOEs are diverse and impactful. One prominent application is in adaptive optics, where LC-based DOEs are used to correct atmospheric distortions in astronomical observations, enabling the capture of sharper images of celestial objects. In free-space optical communication, these DOEs facilitate beam steering, allowing for rapid and precise redirection of laser beams for point-to-point communication and data transfer [142–146]. Additionally, LC-based DOEs find use in variable-focus lenses for imaging devices, such as smartphones and digital cameras, providing dynamic and rapid focusing

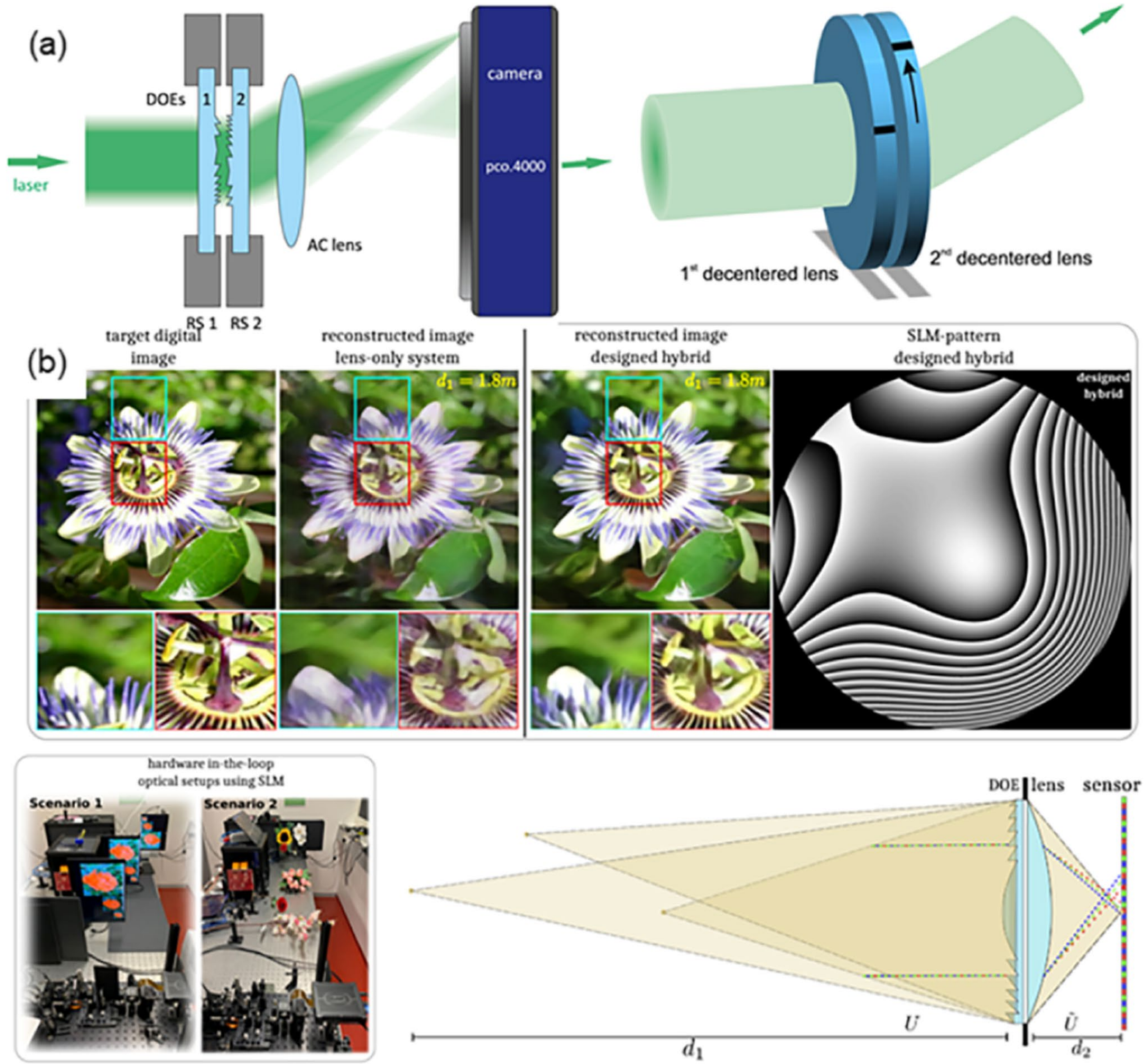

Fig. 8 DOEs for effective optical metrology (**a**) Dynamic beam-steering by a pair of rotating diffractive elements to control viewing direction on camera (Adopted from [26], Figure 1 and 3) (b) DOE exploited for achromatic extended-depth-of-field imaging (Adopted from [131], Figure 1, 3, and 5)

capabilities. Moreover, LC-based DOEs are essential in emerging technologies like augmented reality (AR) and virtual reality (VR) headsets, where they enable adjustable optical elements to achieve immersive and comfortable user experiences. LC-based beam steering is valuable in lidar systems for autonomous vehicles, enhancing 3D mapping and obstacle detection [147–150]. Furthermore, LC-based DOEs have applications in tunable spectral filters, spatial light modulators, and holography, contributing to advancements in spectroscopy, optical signal processing, and 3D display technologies [21].

3.2 Active Modulation of Geometrical Shape

The modulation of geometrical shapes in tunable Diffractive Optical Elements (DOEs) represents a versatile approach for dynamic control over optical wavefronts and beam manipulation. This modulation is achieved through two primary methods: adjusting the gap between the DOE zones or dynamically changing the surface shape. The principle of gap modulation involves altering the spacing between adjacent DOE elements, effectively changing the phase delay experienced by incident light. Alternatively, dynamic

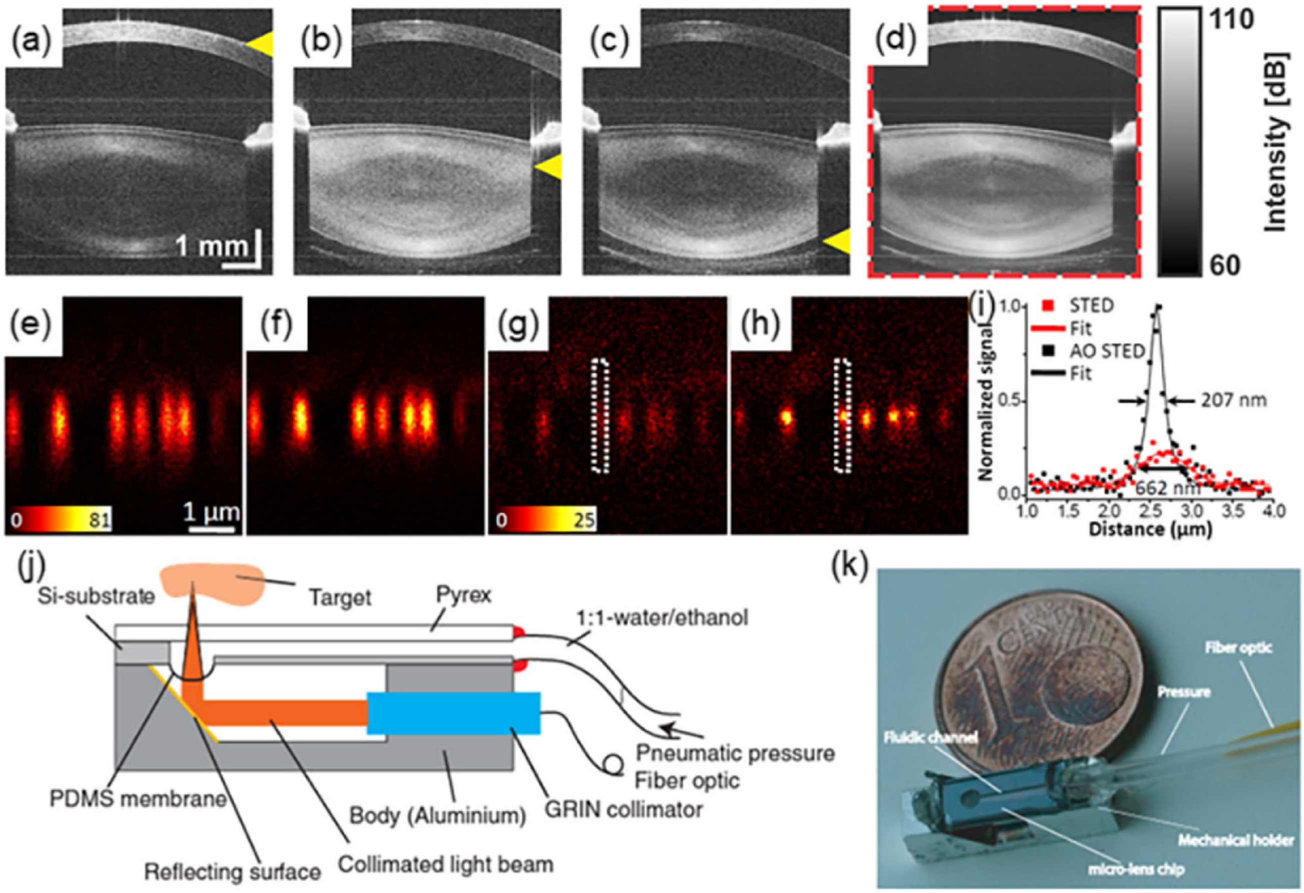

Fig. 9 **a**, **b**, **c**) Anterior segment OCT images for different electrical tunable lens (ETL) current values (focus position indicated by yellow triangle) and (**d**) composite image generated by stacking cross-sections with 50 different foci (Adopted from [132], figure 5) Image of 100 nm fluorescent beads acquired by confocal microscopy (**e**) before and (**f**) after correction of sample-induced aberration using a spatial light modulator (SLM). Stimulated emission depletion (STED) microscopy images with (**g**) correction to the excitation beam only and (**h**) correction to both excitation and depletion beam paths. (**i**) Axial line profiles of dashed boxes in (**g**) and (**h**) in the horizontal direction (Adopted from [133], figure 4) (**j**) Schematic illustration and (**k**) picture of the endoscopic OCT probe with a microfluidic lens (Adopted from [27], figure 12)

surface shape modulation encompasses physically deforming the DOE surface to induce desired phase shifts, enabling real-time optical adjustments. For the medium employed in these tunable DOEs, elastomers and fluids are preferred alternatives due to their ease of actuation and deformation capabilities. Elastomers exhibit mechanical flexibility, enabling precise shape changes with minimal energy input. Fluids, on the other hand, provide adaptability to external forces and can be readily manipulated for shape modulation. Various actuation mechanisms can be employed to drive the tunable DOEs. These include Dielectric Elastomer Actuators (DEAs), piezoelectric elements, external fluid pumps, electromagnetic actuation, electrostatic actuation, and electrothermal effects. DEAs offer rapid and reversible deformations when subjected to an electric field, making them suitable for real-time optical adjustments. Piezoelectric elements provide precise and predictable shape changes in response to voltage inputs, ensuring accurate optical control. External fluid pumps introduce controlled pressure changes to deform the DOE surface. Electromagnetic, electrostatic, and electrothermal actuation methods leverage electromagnetic fields, electric charges, and thermal effects, respectively, to induce surface deformations, offering diverse options for achieving tunable DOEs. Applications of these tunable DOEs facilitate multiple domains, including adaptive optics for astronomical observations, beam shaping and steering in laser processing, variable-focus lenses in imaging devices, and reconfigurable optical systems for telecommunications.

3.3 Active Modulation of the Material Bandgap

Graphene, known for its exceptional electrical, optical, and mechanical properties, serves as an electrically controlled THz modulator through bandgap modulation. Its optical absorption behavior includes dominant interband transitions in the optical and near-infrared spectrum, along with intraband transitions in the far-infrared and terahertz range. This versatility allows graphene to find applications in various terahertz technologies, enabling modulation, detection, and ultrafast carrier recombination. Notably, the material's optical response can be dynamically tailored by adjusting its Fermi level through electrical, optical, or chemical means. By leveraging the field-effect configuration in semiconductors, graphene enables precise control of electron and hole concentrations, with the choice of gate dielectric significantly impacting the operational speed of the device.

These electrically controlled modulators offer a means to observe and manipulate changes across the THz spectrum. In one such instance, Sensale-Rodriguez et al. demonstrated a tunable terahertz modulator using monolayer graphene based on intraband absorption [120]. The device achieved a spectrally-flat intensity modulation of approximately 15% in the frequency range of 570–630 GHz with an insertion loss of about 0.2 dB and a modulation frequency of around 20 kHz, surpassing the performance of AlGaAs/GaAs-based devices. Modifications using a reflection geometry further enhanced the modulation depth to approximately 64% with an insertion loss of roughly 2 dB. The back-gate electrode's role as a reflecting layer enabled enhanced modulation depth at room temperature. In another study, Ju et al. showcased the potential of graphene in terahertz modulation through tunable plasmons in patterned graphene nanoribbons [151]. Their work emphasized the material's capability to couple terahertz waves into subwavelength charge-density oscillations with polarization-sensitive behavior. Additionally, Lee et al. introduced a graphene-metamaterial integrated device capable of both amplitude and phase modulation, achieving a maximum amplitude modulation depth of 47% at resonance [152]. The use of multilayer graphene (MLG) film further increased the modulation depth, showcasing the practical application of these electrically controlled modulators in observing and manipulating changes across the THz spectrum.

With advancements in amplitude and phase modulation, and the establishment of multidimensional arrays, terahertz spatial modulators can now effectively adjust focal length, enable beam steering, and facilitate wavefront shaping. This breakthrough is underpinned by the utilization of graphene for the electric control of the bandgap, thus enabling spatial modulation. Various techniques, including chemical doping and external bias voltage, have been instrumental in achieving substantial modulation depths. For instance, one method involved the segmentation of graphene into a 4×4-pixel array utilizing oxygen plasma, resulting in a notable 50% modulation depth with voltage variations [153]. Furthermore, the application of an ionic liquid electrolyte gating technique led to the development of a transmissive graphene spatial light modulator (SLM) capable of achieving an impressive modulation depth of 80% at 1 THz, maintaining 10% at 1 kHz [154]. Similarly, a graphene metasurface demonstrated the potential for dynamic phase modulation alongside variations in carrier concentration, enabling dynamic beam scanning at 0.98 THz through precise bias distribution [155]. Despite challenges associated with the production of large-area and uniform graphene films, the prospects for utilizing graphene as a spatial modulator remain exceptionally promising.

4 Representative Applications of Tunable Planar Optics

In this chapter, the six potential applications of tunable planar optics have been discussed, particularly space optics, smart photovoltaics, smart window, laser machining, optical metrology, and biomedical imaging.

4.1 Space optics

Application in space typically requires more endeavors than on the ground. The same has been applied to the tunable planar optics. The harsh space environment has hindered its active implementations despite its potential to benefit various space technologies. The optical elements must endure adversarial space environments, such as vacuum, radiation, and dynamic temperature cycles. However, as inter-satellite optical communication has drawn attention and small satellites are prevalent more than ever, tunable optics have been researched for application in space. Compared to conventional optical communication payloads, which require volumetric mechanical actuators for beam steering, tunable optics can usher into optical communication in small satellites. The authors of [123] demonstrated that the liquid lens could endure the vacuum environment. Two types of commercial-off-the-shelf liquid lenses were confirmed to operate normally in a soft vacuum environment. Specifically, an electrowetting-type liquid lens demonstrated almost identical performance under the harsh environment as in ambient conditions. While a pressure-driven liquid lens initially experienced air bubbles, it ultimately performed similarly to ambient conditions after several weeks in the vacuum. The experiment results allude to its possibility of being adopted in space technologies. Since the properties of diffractive planar optics could become advantages in the space development field, diffractive optics have been applied to imaging systems of satellites or surveyors. For common refractive optics, it is essential to increase the diameter of the lens for capturing high-resolution images. However, increased mass and volume of optics require higher launch costs. To reduce the weight and the volume of optics and achieve a speedy system, an alternative method that replaces moving optics by conventional gimbals with light-weight carbon fiber reinforced polymer (CFRP) variable radius-of-curvature mirrors (VRMs) and MEMS deformable mirrors (DMs) was proposed [124]. Just by operating the actuation of the mirrors, the focal lengths and the magnification of the entire system can be adjusted without huge movement of conventional mechanical parts. With an experimental setup that consists of micromachined deformable membrane mirrors and static spherical mirrors, the entire system achieved 4X magnification with an increase of resolution of 2X by adjusting the actuation of mirrors. Since lightweight thin planar optics lack structural stability and rigidity, they are easily affected and corroded by hazard space environments. Active optics with segment mirrors can instead be used to compensate for deformation induced by gravity and to correct low-order aberrations because of temperature change and gravity gradient [22]. To realize active optics, many kinds of actuation are being developed, one of the examples is using a whiffletree-supported mirror. A prototype of 0.676 m diameter is supported by 9 axial and 3 lateral supports, and they serve as hard points. Also, the locations of 9 actuators are selected by solving least squares considering the deformation of mirrors measured by the Fizeau interferometer and bonding interface between mirror and supports. Actuators act along the optical axis of mirrors as push–pull style actuators do. Several tests for correcting gravity-gradient and thermal change are conducted and some Zernike terms (which represent deformation on the unit disk) are corrected by actuators. Follow-up research is progressing to correct more Zernike terms. The results from the performance test promise the ability of such hybrid support to compensate for unexpected deformation and validation of space-active optics. Diffractive Optical Elements (DOEs) are utilized for observing astrophysical phenomena, including but not limited to solar flare observations. For example, aboard the CORONAS-PHOTON satellite, the RT-2/CZT payload was launched into Low Earth Orbit (LEO) in 2009 [125]. Four configurations constituted the payload, two of which used Fresnel Zone Plates (FZPs). Along with a Cadmium Zinc Telluride (CZT) and a Complementary Metal Oxide Semiconductor (CMOS) as detectors, the FZPs were leveraged as shadow-casters for indirect imaging that enables imaging of solar flares in hard X-rays. The simulation demonstrated that the configuration of dual FZPs and a CMOS detector could accomplish an angular resolution of 54 arcseconds with a field-of-view of 4.29 degrees. The performance was sufficient to embrace the full Sun with the finest angular resolution among the four configurations.

4.2 Smart Photovoltaics

Diffractive Optical Elements (DOEs) are widely utilized to revolutionize the field of smart photovoltaics, offering a dynamic solution for optimizing solar energy harvesting. These versatile optical elements enable several key functionalities, including dynamic light management within solar panels and concentrator photovoltaic systems [126, 156–161]. By precisely adjusting the optical properties of the DOE, such as focal length, phase profile, or diffraction pattern, incident sunlight can be expertly steered and concentrated onto photovoltaic cells. This enhances energy collection, particularly in scenarios where sunlight angles vary or sun tracking isn't practical [24, 127, 128, 162–165]. Additionally, tunable DOEs can control the spectral distribution of light, customize the photovoltaic response, improve optical efficiency, and selectively filter out unwanted components. They also play a pivotal role in adaptive solar tracking, ensuring optimal energy conversion. These capabilities make electrically tunable DOEs a promising technology for the advancement of smart photovoltaic systems and the efficient utilization of renewable solar energy.

4.3 Smart Window

Smart windows constitute a critical frontier in the field of building technologies, necessitating specific requirements, offering notable advantages, and inspiring evolving research trends. These windows must possess precise and rapid tunability over their optical properties, enabling dynamic control of light transmission, solar heat gain, and privacy levels. DOEs can offer a versatile and transformative solution for smart window applications. These DOEs can dynamically control the transmission and scattering of light, enabling a range of benefits. They allow for precise regulation of light and heat entering buildings, enhancing comfort and energy efficiency [166, 167]. Variable light transmission and glare reduction ensure occupants can tailor natural lighting while mitigating discomfort from excessive brightness. Privacy control is customizable, with the DOE altering its diffraction pattern to provide both privacy and diffused natural light [168, 169]. Moreover, energy-efficient heating, cooling, and lighting systems are optimized through real-time adjustments, contributing to reduced energy consumption and lower utility costs. Adaptive daylighting solutions and security features enhance overall building functionality and occupant well-being. Additionally, the integration of energy harvesting capabilities further enhances the energy efficiency of smart windows [170–172]. These combined advantages make electrically tunable DOEs a pivotal technology for smart building designs and energy-conscious environments.

Furthermore, energy-efficient smart lighting necessitates the integration of high-efficiency light sources, such as LEDs, and advanced directional light-control technologies to optimize energy consumption and lighting quality [173, 174]. Advantages encompass substantial energy savings, prolonged luminaire lifespan, improved visual comfort, and potential health and well-being benefits through tunable color temperature and intensity. Current research trends focus on enhancing the energy efficiency of smart lighting by developing novel materials, such as perovskite-based LEDs, and integrating IoT (Internet of Things) connectivity for real-time monitoring and control [129, 175–177]. Additionally, research is exploring human-centric lighting solutions that consider circadian rhythms and user preferences, driving the evolution of energy-efficient smart lighting toward more sustainable and user-centric illumination strategies in various applications, from homes to commercial spaces.

4.4 Laser Machining

Electrically tunable Diffractive Optical Elements (DOEs) have become an indispensable property in the realm of laser machining, significantly expanding the capabilities of laser-based manufacturing processes. These versatile optical elements offer a wide range of advantages that enhance precision, productivity, and energy efficiency across various applications. One of the key roles of tunable DOEs in laser machining is beam shaping. They can reshape the typically Gaussian beam profiles generated by lasers into desired intensity distributions, such as top-hat or donut shapes. This transformation ensures uniform energy delivery to the workpiece, resulting in consistent and high-quality machining outcomes. Whether it's cutting, engraving, or surface treatment, the ability to precisely tailor the laser beam profile is invaluable [130, 178–182]. Beam splitting is another crucial function facilitated by tunable DOEs. These optical elements allow a single laser beam to be split into multiple beams with precise control over their distribution. This capability is especially beneficial for parallel processing, where multiple workpieces or features can be machined simultaneously, significantly improving productivity and throughput [25, 183–185]. Furthermore, tunable DOEs offer the advantage of focal length control without the need for physical adjustments in the distance between the laser source and the workpiece. This dynamic focal length modification proves particularly useful in scenarios where different machining tasks require varying focus settings. It simplifies and streamlines the machining process while maintaining precision [119, 122, 186]. Real-time dynamic beam steering is another hallmark feature of tunable DOEs, allowing for the precise control of laser beam direction by adjusting phase shifts across the surface of the DOE. This dynamic beam steering capability is valuable in material ablation and cutting processes, especially in applications where rapid and precise beam positioning is essential for achieving intricate patterns or complex geometries [26, 187]. Moreover, these DOEs provide a high level of customization and flexibility, accommodating various laser machining tasks and seamlessly integrating into different laser systems, thereby meeting the diverse needs of contemporary laser-based manufacturing.

4.5 Optical Metrology

Electrically tunable Diffractive Optical Elements (DOEs) have established themselves as indispensable tools in the field of optical metrology, offering an extensive range of capabilities that enhance precision, versatility, and adaptability in a wide array of applications. Dynamic focusing is one of the primary functions that tunable DOEs excel at in optical metrology. They empower users with dynamic control over the focus and depth of field of laser beams, a crucial aspect for metrology applications that involve the measurement of 3D surfaces or complex geometries [188–190]. By carefully adjusting the DOE, the laser focus can be meticulously tailored to different surface profiles, ensuring that measurements are not only precise but also highly accurate, regardless of the intricacies of the target surface. Additionally, tunable DOEs facilitate high-precision laser interferometry, supporting distance, displacement, and vibration measurements. They play a key role in surface defect detection, projecting structured light for identifying flaws and irregularities [131, 191]. These DOEs contribute to accurate distance measurements in laser distance systems and enhance surface roughness assessment. In non-destructive testing, they assist in generating controlled laser-induced ultrasonic waves [26, 192, 193]. Their adaptability and real-time adjustments make them valuable in dynamic metrology tasks, promising continued advancements in the field.

4.6 Biomedical Imaging

Tunable optics, which allow for real-time control of optical parameters, have found diverse applications in bio-imaging. From optical coherence tomography (OCT) to super-resolution microscopy, their ability to manipulate focal planes and enhance imaging quality has greatly enhanced our understanding of biological structures and functions [132, 133, 194–196]. In particular, endoscopic OCT, with its potential for diagnosing luminal organs such as arteries and esophagus [197, 198], faces technical challenges due to its static and limited depth of field. To address these limitations, researchers have explored methods to dynamically control the focal length of optics [199, 200]. A notable example is the use of tunable microfluidic lenses [27, 201]. These lenses adjust their focal length dynamically by manipulating the shape of a liquid-filled chamber, providing a compact alternative to traditional, bulky lens systems. Nevertheless, introducing microfluidic lenses to endoscopic instruments presents challenges, including manufacturing complexity, durability, and precise control of lens properties. Additionally, there is growing interest in incorporating micro-electro-mechanical systems (MEMS) into endoscopic instruments [202–204]. While MEMS technology allows for miniaturized optical components with dynamic capabilities in line with the goals of tunable optics, it also encounters issues related to manufacturing complexity and cost-effectiveness. Tunable planar optics emerge as a promising alternative that might effectively address these obstacles. The flat and flexible structure of the tunable planar optics simplifies manufacturing processes and reduces production costs. Moreover, these optics can offer precise control of optical parameters, thus making them suitable for dynamic adjustments during endoscopic procedures. Consequently, the substitution of traditional bulky optics with thin and light-weight tunable planar counterparts can make endoscopic devices more agile, less invasive, and ultimately more patient-friendly.

5 Summary and Future Prospects

This review has investigated the design, green manufacturing, and application of electrically-tunable smart lightweight planar optics. Direct laser writing, with its distinct advantages, emerges as a key technique that minimizes the environmental impact compared to traditional methods, aligning with the growing emphasis on sustainability in manufacturing. DLW offers design flexibility, enabling precise control and various designs for tunable Diffractive Optical Elements (DOE). Its facile process eliminates the need for multiple steps and hazardous chemicals, significantly reducing environmental impact. DLW's chemical-free, energy-efficient operation aligns perfectly with green manufacturing principles, making it an ideal choice for sustainable fabrication of tunable DOE. Moreover, electrically-tunable planar optics can be realized by active modulation of refractive index, geometrical shape, and bandgap. The capability to tailor these optical elements' focal length, aberration, transparency, and beam propagation angle is opening up new possibilities in space optics, photovoltaics, mobile phone lenses, and beyond.

In moving toward the future, the evolution of electrically-tunable smart lightweight planar optics hinges on three crucial avenues for exploration. Firstly, there is a need to broaden the spectrum of modulation materials, expanding beyond the current candidates such as graphene, MoS_2, and MXene [205–209]. This exploration should consider materials not only for their tunability but also for compatibility with eco-friendly manufacturing processes. Secondly, the refinement of modulation techniques, encompassing advancements in precision, efficiency, and scalability, is essential for electrically-tunable planar optics. Lastly, the practical application of tunable diffractive optical elements (DOEs) across diverse fields, from space optics to biomedical imaging, requires research regarding real-world implementations. By addressing these requirements, this research field can be impelled forward, unlocking the full potential of tunable DOEs and facilitating a new era of versatile and sustainable optical solutions.

Acknowledgements This work received support from the National Research Foundation of Korea (NRF) through grants NRF-2021R1A4A103166013, NRF-2020R1A2C210233813, and NRF-2012R1A3A105038626, as well as from the Korea Forest Service (KFS) under grant KOFPI-2020229C10-2222-AC01, and the Ministry of Agriculture, Food and Rural Affairs (MAFRA) under grant IPET-321077022SB010, also funded by Basic Research Program of Korea Institute of Machinery and Materials (NK248B).

Funding Open Access funding enabled and organized by KAIST.

Data Availability The data that supports the findings of this research are available and can be accessed upon request. Please contact the authors for data inquiries.

Declarations

Conflict of Interest The authors declare that they have no known competing financial interests or personal relationships that could have appeared to influence the work reported in this paper.

Open Access This article is licensed under a Creative Commons Attribution 4.0 International License, which permits use, sharing, adaptation, distribution and reproduction in any medium or format, as long as you give appropriate credit to the original author(s) and the source, provide a link to the Creative Commons licence, and indicate if changes were made. The images or other third party material in this article are included in the article's Creative Commons licence, unless indicated otherwise in a credit line to the material. If material is not included in the article's Creative Commons licence and your intended use is not permitted by statutory regulation or exceeds the permitted use, you will need to obtain permission directly from the copyright holder. To view a copy of this licence, visit http://creativecommons.org/licenses/by/4.0/.

References

1. Hasman, E., Davidson, N., Danziger, Y., & Friesem, A. A. (1997). Diffractive optics: Design, realization, and applications. *Fiber and Integrated Optics, 16*(1), 1–25.
2. Huang, K., Qin, F., Liu, H., Ye, H., Qiu, C. W., Hong, M., Luk'yanchuk, B., Teng, J. (2018). Planar diffractive lenses: Fundamentals, functionalities, and applications. *Advanced Materials*, *30*(26), 1–22.
3. Kiss, M., Mi, S., Huszka, G., & Quack, N. (2021). Diamond diffractive optics - Recent progress and perspectives. *Advanced Optical Technologies, 10*(1), 19–30.
4. Oscurato, S. L., Reda, F., Salvatore, M., Borbone, F., Maddalena, P., & Ambrosio, A. (2022). Shapeshifting diffractive optical devices. *Laser & Photonics Reviews, 16*(4), 1–10.
5. Lee, Y., Low, M. J., Yang, D., Nam, H. K., Le, T. S. D., Lee, S. E., Han, H., Kim, S., Vu, Q. H., Yoo, H., Yoon, H., Lee, J., Sandeep, S., Lee, K., Kim, S. W., Kim, Y. J. (2023). Ultra-thin light-weight laser-induced-graphene (LIG) diffractive optics. *Light: Science & Applications, 12*(1), 146.

6. Danilov, V. A. (2022). Laser Technology and nanotechnology applying diffractive optical elements. *Nanobiotechnology Reports, 17*(6), 747–757.
7. Hu, Z. Y., Jiang, T., Tian, Z. N., Niu, L. G., Mao, J. W., Chen, Q. D., & Sun, H. B. (2022). Broad-bandwidth micro-diffractive optical elements. *Laser & Photonics Reviews, 16*(3), 1–8.
8. Guidry, A., Kyrish, M., Stone, L., Fraelich, M., Lechuga, O., Claytor, N. (2020). Distinguishing characteristics of diffractive optical elements and Fresnel lenses. *11487*, 1148715.
9. Orange-Kedem, R., Nehme, E., Weiss, L. E., Ferdman, B., Alalouf, O., Opatovski, N., & Shechtman, Y. (2021). 3D printable diffractive optical elements by liquid immersion. *Nature Communications, 12*(1), 1–6.
10. Fu, R., Chen, K., Li, Z., Yu, S., & Zheng, G. (2022). Metasurface-based nanoprinting: Principle, design and advances. *Opto-Electronic Science, 1*(10), 220011–220011.
11. Qiu, C. W., Zhang, T., Hu, G., & Kivshar, Y. (2021). Quo vadis, metasurfaces? *Nano Letters, 21*(13), 5461–5474.
12. Hsiao, H. H., Chu, C. H., & Tsai, D. P. (2017). Fundamentals and applications of metasurfaces. *Small Methods, 1*(4), 1–20.
13. Jiang, Q., Jin, G., & Cao, L. (2019). When metasurface meets hologram: Principle and advances. *Advances in Optics and Photonics, 11*(3), 518.
14. Huang, L., Zhang, S., & Zentgraf, T. (2018). Metasurface holography: From fundamentals to applications. *Nanophotonics, 7*(6), 1169–1190.
15. Hu, J., Bandyopadhyay, S., Liu, Y. H., & Shao, L. Y. (2021). A review on metasurface: From principle to smart metadevices. *Frontiers of Physics, 8*, 1–20.
16. Jester, T. L. (2002). Crystalline silicon manufacturing progress. *Progress in Photovoltaics: Research and Applications, 10*(2), 99–106.
17. Franke, D., Rettelbach, T., Häßler, C., Koch, W., & Müller, A. (2002). Silicon ingot casting: Process development by numerical simulations. *Solar Energy Materials and Solar Cells, 72*(1–4), 83–92.
18. Yoon, C., Kim, S., Park, D., Choi, Y., Jo, J., & Lee, K. (2020). Chemical use and associated health concerns in the semiconductor manufacturing industry. *Safety and Health at Work, 11*(4), 500–508.
19. Eom, Y. S., Hong, J. H., Lee, S. J., Lee, E. J., Cha, J. S., Lee, D. G., & Bang, S. A. (2006). Emission factors of air toxics from semiconductor manufacturing in Korea. *Journal of the Air and Waste Management Association, 56*(11), 1518–1524.
20. Klein, L. C. (2019). *Sol-Gel Glasses*. In J. D. Musgraves, J. Hu, & L. Calvez (Eds.), *Springer Handbook of Glass*. Cham: Springer Handbooks, Springer.
21. Schmitz, A., Kamiński, J., Scalet, B. M, Soria A. (2011) Energy consumption and CO2 emissions of the European glass industry. Energy Policy, *39*(1), 142–155.
22. Zhou, P., Zhang, D., Liu, G., & Yan, C. (2019). Development of space active optics for a whiffletree supported mirror. *Applied Optics, 58*(21), 5740.
23. Chowdhary, A. K., & Sikdar, D. (2021). Design of electrotunable all-weather smart windows. *Solar Energy Materials & Solar Cells, 222*, 110921
24. Mohammad, N., Wang, P., Friedman, D. J., & Menon, R. (2014). Enhancing photovoltaic output power by 3-band spectrum-splitting and concentration using a diffractive micro-optic. *Optics Express, 22*(S6), A1519.
25. Kuchmizhak, A. A., Porfirev, A. P., Syubaev, S. A., Danilov, P. A., Ionin, A. A., Vitrik, O. B., Kulchin, Y. N., Khonina, S. N., & Kudryashov, S. I. (2017). Multi-beam pulsed-laser patterning of plasmonic films using broadband diffractive optical elements. *Optics Letters, 42*(14), 2838–2841.
26. Bawart, M., Bregenzer, N., Bernet, S., & Ritsch-Marte, M. (2020). Dynamic beam-steering by a pair of rotating diffractive elements. *Optics Communication, 460*, 125071.
27. Aljasem, K., Werber, A., Seifert, A., & Zappe, H. (2008). Fiber optic tunable probe for endoscopic optical coherence tomography. *Journal of Optics A: Pure and Applied Optics, 10*(4), 044012.
28. Bernet, S. (2021). Combined diffractive optical elements with adjustable optical properties controlled by a relative rotation: Tutorial. *Journal of the Optical Society of America A. Optics and Image Science, 38*(10), 1521.
29. Chanda, D., & Herman, P. R. (2007). Phase tunable multilevel diffractive optical element based single laser exposure fabrication of three-dimensional photonic crystal templates. *Applied Physics Letters, 91*(6), 061122
30. Bernet, S., Harm, W., Ritsch-marte, M. (2013). Demonstration of focus-tunable diffractive Moir´e-lenses. *21*(6), 6955–6966.
31. Bernet, S., & Ritsch-Marte, M. (2017). Multi-color operation of tunable diffractive lenses. *Optics Express, 25*(3), 2469.
32. Bawart, M., May, M. A., Öttl, T., Roider, C., Bernet, S., Schmidt, M., Ritsch-Marte, M., & Jesacher, A. (2020). Diffractive tunable lens for remote focusing in high-NA optical systems. *Optics Express, 28*(18), 26336.
33. Döring, S., Kollosche, M., Hildebrandt, N., Stumpe, J., Kofod, G. (2010). Tunable diffractive optical elements on various electro active polymers. *Micro-Optics*, *7716*(May 2010), 77160F.
34. David, C., Noehammer, B., Ziegler, E., Hignette, O. (2001). Tunable diffractive optical elements for hard x-rays. *Proc. of SPIE*, *4499*, 96–104.
35. Siemion, A. (2019). Terahertz diffractive optics—Smart control over radiation. *Journal of Infrared, Millimeter, and Terahertz Waves, 40*(5), 477–499.
36. Chen, L., Ghilardi, M., Busfield, J. J. C., & Carpi, F. (2021). Electrically tunable lenses: A review. *Frontiers in Robotics and AI, 8*, 1–20.
37. Sussman, M. (1960). Elementary diffraction theory of zone plates. *American Journal of Physics, 28*(4), 394–398.
38. Cao, Q., & Jahns, J. (2003). Modified Fresnel zone plates that produce sharp Gaussian focal spots. *Journal of the Optical Society of America A. Optics and Image Science, 20*(8), 1576.
39. Pang, H., Yin, S., Deng, Q., Qiu, Q., & Du, C. (2015). A novel method for the design of diffractive optical elements based on the Rayleigh-Sommerfeld integral. *Optics and Lasers in Engineering, 70*, 38–44.
40. Wolf, E., Emil, W., M. (1964). Comparison of the Kirchhoff and the Rayleigh–Sommerfeld theories of diffraction at an aperture. *54*(5), 587–594.
41. Khonina, S. N., Ustinov, A. V., Skidanov, R. V., & Porfirev, A. P. (2015). Local foci of a parabolic binary diffraction lens. *Applied Optics, 54*(18), 5680.
42. Liu, T., Wang, L., Zhang, J., Fu, Q., & Zhang, X. (2018). Numerical simulation and design of an apodized diffractive optical element composed of open-ring zones and pinholes. *Applied Optics, 57*(1), 25.
43. Mehrabkhani, S., & Schneider, T. (2017). Is the Rayleigh-Sommerfeld diffraction always an exact reference for high speed diffraction algorithms? *Optics Express, 25*(24), 30229.
44. Zhao, X., Hu, J., Lin, Y., Xu, F., Zhu, X., Pu, D., Chen, L., & Wang, C. (2016). Ultra-broadband achromatic imaging with diffractive photon sieves. *Science and Reports, 6*, 1–9.
45. Zhang, H., Liu, H., Xu, W., & Lu, Z. (2019). Large aperture diffractive optical telescope: A review. *Optics & Laser Technology, 130*(June), 2020.
46. Zhang, H., Liu, H., Lizana, A., Xu, W., Caompos, J., & Lu, Z. (2017). Methods for the performance enhancement and the error

characterization of large diameter ground-based diffractive telescopes. *Optics Express, 25*(22), 26662.
47. Zhang, B., Piao, M., & Cui, Q. (2019). Achromatic annular folded lens with reflective-diffractive optics. *Optics Express, 27*(22), 32337.
48. He, Y., Zhao, L., Tang, Y., & Hu, S. (2014). A hybrid doubled achromat based on a photon sieve. *Optik (Stuttgart), 125*(3), 958–961.
49. Mun Ji Low, Y.-J. K., Rohith, T. M., Kim, B., Kim, S.-W., Suchand Sandeep, C. S., Murukeshan, V. M. (2022). Refractive-diffractive hybrid optics array: comparative analysis and experiments. *Journal of Optics*, *24*(055401).
50. Jin, G., Yan, J., Liu, H., Zhong, X., & Yan, Y. (2014). Flat-stitching error analysis of large-aperture photon sieves. *Applied Optics, 53*(1), 90–95.
51. Soltau, J., Lohse, L. M., Osterhoff, M., & Salditt, T. (2021). Finite-difference propagation for the simulation of x-ray multilayer optics. *Optics Express, 29*(25), 41932.
52. Döring, F., Robisch, A. L., Eberl, C., Osterhoff, M., Ruhlandt, A., Liese, T., Schlenkrich, F., Hoffmann, S., Bartels, M., Salditt, T., & Krebs, H. U. (2013). Sub-5 nm hard x-ray point focusing by a combined Kirkpatrick-Baez mirror and multilayer zone plate. *Optics Express, 21*(16), 19311.
53. Zemax, R. (2014). Zemax 13 optical design program user's manual. Zemax LLC.
54. Khorasaninejad, M., Chen, W. T., Devlin, R. C., Oh, J., Zhu, A. Y., Capasso, F. (2016). Metalenses at visible wavelengths: Diffraction-limited focusing and subwavelength resolution imaging. *Science (80-.)*, *352*(6290), 1190–1194.
55. Fraser, W., & Ye, W. N. (2023). Silicon metalens using Fresnel zone plate with subwavelength gratings. *Sensors, 23*(8), 4137.
56. Moon, I. Y., Kim, B. H., Lee, H. W., Oh, Y. S., Kim, J. H., & Kang, S. H. (2020). Superhydrophobic polymer surface with hierarchical patterns fabricated in hot imprinting process. *International Journal of Precision Engineering and Manufacturing-Green Technology, 7*(2), 493–503.
57. Roos, M. M., Winkler, A., Nilsen, M., Menzel, S. B., & Strehle, S. (2022). Towards Green 3D-Microfabrication of Bio-MEMS devices using ADEX dry film photoresists. *International Journal of Precision Engineering and Manufacturing-Green Technology, 9*(1), 43–57.
58. Kim, H. C., Zhai, L., Panicker, P. S., Kim, H. J., MacDonnell, D., & Kim, J. (2022). Transparent and flexible photon sieve made with cellulose nanofiber by micro-nano structure molding. *International Journal of Precision Engineering and Manufacturing-Green Technology, 9*(4), 1165–1175.
59. Huang, R., Zhang, X. Q., Ng, B. P., Kumar, A. S., & Liu, K. (2021). Roll-to-roll embossing of optical radial fresnel lenses on polymer film for concentrator photovoltaics: A feasibility study. *International Journal of Precision Engineering and Manufacturing-Green Technology, 8*(1), 77–88.
60. Chien, H. L., & Lee, Y. C. (2020). Three dimensional maskless ultraviolet exposure system based on digital light processing. *International Journal of Precision Engineering and Manufacturing, 21*(5), 937–945.
61. Byiringiro, J. B., Ko, T. J., Kim, H. C., & Lee, I. H. (2013). Optimal conditions of SU-8 mask for micro-abrasive jet machining of 3-D freeform brittle materials. *International Journal of Precision Engineering and Manufacturing, 14*(11), 1989–1996.
62. Yu, J. H., Kang, K. T., Hwang, J. Y., Lee, S. H., & Kang, H. (2014). Rapid sintering of copper nano ink using a laser in air. *International Journal of Precision Engineering and Manufacturing, 15*(6), 1051–1054.
63. Park, J., Shin, K., & Lee, C. (2016). Mechanical aspects of the chemical mechanical polishing process: A review. *International Journal of Precision Engineering and Manufacturing, 17*(4), 537–550.
64. Kim, J. H., Chang, S. S., & Lim, G. (2014). A simple approach for an ultra-precise patterning using deep x-ray lithography with a micron-patterned x-ray mask. *International Journal of Precision Engineering and Manufacturing, 15*(11), 2385–2390.
65. Kim, M. S., & Kim, J. H. (2011). Design of a gain scheduled PID controller for the precision stage in lithography. *International Journal of Precision Engineering and Manufacturing, 12*(6), 993–1000.
66. Terashima, S., Tatsukawa, C., Suzuki, M., Takahashi, T., & Aoyagi, S. (2020). Twice stretched fabrication of polylactic acid microneedle arrays using drawing lithography. *International Journal of Precision Engineering and Manufacturing, 21*(10), 1933–1942.
67. Kang, D. W., Kang, M., & Hahn, J. W. (2015). Keystone error analysis of projection optics in a maskless lithography system. *International Journal of Precision Engineering and Manufacturing, 16*(2), 373–378.
68. Hwang, J., Cho, Y. H., Park, M. S., & Kim, B. H. (2019). Microchannel fabrication on glass materials for microfluidic devices. *International Journal of Precision Engineering and Manufacturing, 20*(3), 479–495.
69. Chen, H. W. (2007). Exposure and health risk of gallium, indium, and arsenic from semiconductor manufacturing industry workers. *Bulletin of Environment Contamination and Toxicology, 78*(2), 113–117.
70. Wang, T., Zhong, S., Luo, H., & Kuang, N. (2023). Drift error calibration method based on Multi-MEMS gyroscope data fusion. *International Journal of Precision Engineering and Manufacturing, 24*(10), 1835–1844.
71. Le, T. S. D., Lee, Y. A., Nam, H. K., Jang, K. Y., Yang, D., Kim, B., Yim, K., Kim, S. W., Yoon, H., & Kim, Y. J. (2022). Green flexible graphene–inorganic-hybrid micro-supercapacitors made of fallen leaves enabled by ultrafast laser pulses. *Advanced Functional Materials, 32*(20), 2107768.
72. Yang, D., Nam, H. K., Le, T.-S.D., Yeo, J., Lee, Y., Kim, Y.-R., Kim, S.-W., Choi, H.-J., Shim, H. C., Ryu, S., Kwon, S., & Kim, Y.-J. (2023). Multimodal e-textile enabled by one-step maskless patterning of femtosecond-laser-induced graphene on nonwoven, knit, and woven textiles. *ACS Nano, 17*, 18893–18904.
73. Donnelly, V. M., Kornblit A. (2013). Plasma etching: Yesterday, today, and tomorrow. *Journal of Vacuum Science and Technology A, 31*(5), 050825.
74. Hwang, E., Lee, Y., Lim, J., Kim, Y., Qu, W., Min, K., Lee, W. C., & Hong, S. (2021). Selective laser pyrolytic micropatterning of stretched elastomeric polymer surfaces. *International Journal of Precision Engineering and Manufacturing-Green Technology, 8*(3), 795–804.
75. Tebaay, L. M., Hahn, M., & Tekkaya, A. E. (2020). Distortion and dilution behavior for laser metal deposition onto thin sheet metals. *International Journal of Precision Engineering and Manufacturing-Green Technology, 7*(3), 625–634.
76. Jeong, S. Y., Sugita, N., & Shin, B. S. (2023). Fe3O4/Laser-induced graphene as an adsorbent for microplastics emitted from household wastewater. *International Journal of Precision Engineering and Manufacturing-Green Technology, 10*(3), 807–818.
77. Lin, B. Q., Huang, C. P., Tian, K. Y., Lee, P. H., Su, W. F., & Xu, L. (2023). Laser patterning technology based on nanosecond pulsed laser for manufacturing bifacial perovskite solar modules. *International Journal of Precision Engineering and Manufacturing-Green Technology, 10*(1), 123–139.
78. Kim, B., Nam, H. K., Watanabe, S., Park, S., Kim, Y., Kim, Y. J., Fushinobu, K., & Kim, S. W. (2021). Selective laser ablation of metal thin films using ultrashort pulses. *International Journal*

of Precision Engineering and Manufacturing-Green Technology, 8(3), 771–782.

79. Nam, J. B., Jang, Y. R., Hwang, Y. T., Kim, H. H., Jung, I. H., & Kim, H. S. (2022). Intense pulsed light sintering of screen-printed paste electrode on silicon solar cell for high throughput and cost-effective low temperature metallization. *International Journal of Precision Engineering and Manufacturing-Green Technology, 9*(2), 523–535.
80. Hwang, Y. T., & Kim, H. S. (2022). The ultrafast and eco-friendly reduction of graphene oxide using a UV–IR assisted intense pulsed light and its application as supercapacitor. *International Journal of Precision Engineering and Manufacturing-Green Technology, 9*(1), 201–211.
81. Chang, C. S., Wu, K. T., Han, C. F., Tsai, T. W., Liu, S. H., & Lin, J. F. (2022). Establishment of the model widely valid for the melting and vaporization zones in selective laser melting printings via experimental verifications. *International Journal of Precision Engineering and Manufacturing-Green Technology, 9*(1), 143–162.
82. Yamamuro, Y., Shimoyama, T., & Yan, J. (2022). Microscale surface patterning of zirconia by femtosecond pulsed laser irradiation. *International Journal of Precision Engineering and Manufacturing-Green Technology, 9*(2), 619–632.
83. Le, T. S. D., Lee, Y. A., Nam, H. K., Jang, K. Y., Yang, D., Kim, B., Yim, K., Kim, S. W., Yoon, H., & Kim, Y. J. (2022). Green flexible graphene–inorganic-hybrid micro-supercapacitors made of fallen leaves enabled by ultrafast laser pulses. *Advanced Functional Materials, 32*(20), 1–12.
84. Le, T. S. D., Phan, H. P., Kwon, S., Park, S., Jung, Y., Min, J., Chun, B. J., Yoon, H., Ko, S. H., Kim, S. W., & Kim, Y. J. (2022). Recent advances in laser-induced graphene: mechanism, fabrication, properties, and applications in flexible electronics. *Advanced Functional Materials, 32*(48), 1–39.
85. Nam, H. K., Le, T. S. D., Yang, D., Kim, B., Lee, Y., Hwang, J. S., Kim, Y. R., Yoon, H., Kim, S. W., & Kim, Y. J. (2023). Smart wooden home enabled by direct-written laser-induced graphene. *Advanced Materials Technologies, 2201952*(8), 1–9.
86. Ye, R., Chyan, Y., Zhang, J., Li, Y., Han, X., Kittrell, C., & Tour, J. M. (2017). Laser-induced graphene formation on wood. *Advanced Materials, 29*(37), 1–7.
87. Jayan, J. S., & Jayan, S. S. (2023). Biomass-derived laser-induced graphene and its advances in the electronic applications. *Advanced Engineering Materials, 25*(16), 1–16.
88. Le, T. S. D., Park, S., An, J., Lee, P. S., & Kim, Y. J. (2019). Ultrafast laser pulses enable one-step graphene patterning on woods and leaves for green electronics. *Advanced Functional Materials, 29*(33), 1–10.
89. Kim, Y. J., Le, T. S. D., Nam, H. K., Yang, D., & Kim, B. (2021). Wood-based flexible graphene thermistor with an ultra-high sensitivity enabled by ultraviolet femtosecond laser pulses. *CIRP Annals, 70*(1), 443–446.
90. Kim, Y. J., Yang, D., Nam, H. K., Le, T. S. D., Lee, Y., & Kwon, S. (2022). Direct-laser-conversion of Kevlar textile to laser-induced-graphene for realizing fast and flexible fabric strain sensors. *CIRP Annals, 71*(1), 473–476.
91. Hwang, J. S., Arthanari, S., Park, J. E., Yang, M., Kim, S., Kim, S. W., Lee, H., & Kim, Y. J. (2022). One-step template-free laser patterning of metal microhoneycomb structures. *Small Methods, 6*(5), 1–8.
92. Park, S. H., Choi, S., & Jhang, K. Y. (2022). Porosity evaluation of additively manufactured components using deep learning-based ultrasonic nondestructive testing. *International Journal of Precision Engineering and Manufacturing-Green Technology, 9*(2), 395–407.
93. Gao, M., Li, L., Wang, Q., Ma, Z., Li, X., & Liu, Z. (2022). Integration of additive manufacturing in casting: Advances, challenges, and prospects. *International Journal of Precision Engineering and Manufacturing-Green Technology, 9*(1), 305–322.
94. Szkodo, M., Bień, A., & Stanisławska, A. (2022). Laser beam as a precision tool to increase fatigue resistance in an eyelet of undercarriage drag strut. *International Journal of Precision Engineering and Manufacturing-Green Technology, 9*(1), 175–190.
95. Ma, Y. W., Park, J. H., Lee, S. J., Lee, J., Cho, S., & Shin, B. S. (2023). Fabrication system for large-area seamless nanopatterned cylinder mold using the spiral laser interference exposure method. *International Journal of Precision Engineering and Manufacturing-Green Technology, 10*(1), 1–7.
96. Sun, L., Ren, X., He, J., & Zhang, Z. (2022). Melting cell based compensated design method for improving dimensional accuracy of additively manufactured thin channels. *International Journal of Precision Engineering and Manufacturing-Green Technology, 9*(2), 383–394.
97. Nakajima, A., & Yan, J. (2022). Response of resin coating films containing fine metal particles to ultrashort laser pulses. *International Journal of Precision Engineering and Manufacturing, 23*(4), 385–393.
98. Low, M. J., Rohith, T. M., Kim, B., Kim, S. W., Suchand Sandeep, C. S., Murukeshan, V. M., Kim, Y. J. (2022). Refractive-diffractive hybrid optics array: Comparative analysis of simulation and experiments. *Journal of Optics*, *24*(5), 055401.
99. Low, M. J., Lee, H., Lim, C. H. J., Suchand Sandeep, C. S., Murukeshan, V. M., Kim, S. W., & Kim, Y. J. (2020). Laser-induced reduced-graphene-oxide micro-optics patterned by femtosecond laser direct writing. *Applied Surface Science, 526*(February), 146647.
100. Choi, H. J., Cho, C., Woo, S., Lee, J. Y., Yoo, Y. E., Jeon, M., Kim, G. H., Je, T. J., & Chae Jeon, E. (2021). Manufacturing of compound parabolic concentrator devices using an ultra-fine planing method for enhancing efficiency of a solar cell. *International Journal of Precision Engineering and Manufacturing-Green Technology, 8*(5), 1405–1414.
101. Liu, Y., Shang, S., Mo, S., Wang, P., & Wang, H. (2021). Eco-friendly strategies for the material and fabrication of wearable sensors. *International Journal of Precision Engineering and Manufacturing-Green Technology, 8*(4), 1323–1346.
102. Ho, C. M. B., Hu, K., Mishra, A., Noh, J., Kim, J., Lee, S., Yoon, M. S., & Yoon, Y. J. (2022). Printing of woodpile scaffold using fresnel lens for tissue engineering. *International Journal of Precision Engineering and Manufacturing-Green Technology, 9*(2), 507–522.
103. Liu, X., Mo, R., Li, K., Shen, J., Ma, J., & Gong, F. (2021). Manufacturing of 3D microlens array mold on bulk metallic glass by self-aligned multi-ball hot embossing. *International Journal of Precision Engineering and Manufacturing-Green Technology, 8*(4), 1209–1223.
104. Lee, C., Kim, S., Jo, M., & Lee, J. (2021). Residual interfacial deformation in flexible copper clad laminate occurring during roll-to-roll composite film manufacturing. *International Journal of Precision Engineering and Manufacturing-Green Technology, 8*(3), 805–815.
105. Kang, B., Sung, J., & So, H. (2021). Realization of superhydrophobic surfaces based on three-dimensional printing technology. *International Journal of Precision Engineering and Manufacturing-Green Technology, 8*(1), 47–55.
106. Koo, S., Lee, S. H., Kim, J. D., Hong, J. G., Baac, H. W., Kwak, M. K., & Ok, J. G. (2016). Controlled airbrush coating of polymer resists in Roll-to-Roll nanoimprinting with regimented residual layer thickness. *International Journal of Precision Engineering and Manufacturing, 17*(7), 943–947.

107. Nguyen, H. A. D., Shin, K., & Lee, C. (2015). Effect of nip force on ink transfer in high resolution roll-to-roll printing. *International Journal of Precision Engineering and Manufacturing, 16*(3), 517–523.
108. Seong, J., Kim, S., Park, J., Lee, D., & Shin, K. H. (2015). Online noncontact thickness measurement of printed conductive silver patterns in Roll-to-Roll gravure printing. *International Journal of Precision Engineering and Manufacturing, 16*(11), 2265–2270.
109. Kang, H., & Lee, C. (2015). Effect of tension on conductivity of gravure printed Ag layer in roll-to-roll process. *International Journal of Precision Engineering and Manufacturing, 16*(1), 99–104.
110. Park, J., Shin, K., & Lee, C. (2015). Improvement of cross-machine directional thickness deviation for uniform pressure-sensitive adhesive layer in roll-to-roll slot-die coating process. *International Journal of Precision Engineering and Manufacturing, 16*(5), 937–943.
111. Costner, E. A., Lin, M. W., Jen, W. L., & Willson, C. G. (2009). Nanoimprint lithography materials development for semiconductor device fabrication. *Annual Review of Materials Research, 39*, 155–180.
112. Dore, C., Osmond, J., & Mihi, A. (2018). A water-processable cellulose-based resist for advanced nanofabrication. *Nanoscale, 10*(37), 17884–17892.
113. Yu, C. C., & Chen, H. L. (2015). Nanoimprint technology for patterning functional materials and its applications. *Microelectronic Engineering, 132*, 98–119.
114. Auner, C., Palfinger, U., Gold, H., Kraxner, J., Haase, A., Haber, T., Sezen, M., Grogger, W., Jakopic, G., Krenn, J. R., Leising, G., & Stadlober, B. (2009). Residue-free room temperature UV-nanoimprinting of submicron organic thin film transistors. *Organic Electronics, 10*(8), 1466–1472.
115. Oh, J., Hoffman, J. B., Hong, S., Jo, K. D., Román-Kustas, J., Reed, J. H., Dana, C. E., Cropek, D. M., Alleyne, M., & Miljkovic, N. (2020). Dissolvable template nanoimprint lithography: A facile and versatile nanoscale replication technique. *Nano Letters, 20*(10), 6989–6997.
116. Hanabata, M., Takei, S., Sugahara, K., Nakajima, S., Sugino, N., Kameda, T., Fukushima, J., Matsumoto, Y., & Sekiguchi, A. (2016). Nanoimprint lithography using disposable biomass template. *SPIE Photonics Europe, 9777*, 97771G.
117. Matsumoto, Y., Sekiguchi, A., Nakajima, S., Takei, S., Hanabata, M., Sugino, N., & Kameda, T. (2017). High resolution patterning of ultraviolet cross-linked resins using gas permeable mold derived from cellulose in nanoimprint lithography. *SPIE Photonics Europe, 10354*, 47.
118. Jo, M., Kim, S., & Lee, C. (2022). Morphology engineering for compact electrolyte layer of solid oxide fuel cell with roll-to-roll eco-production. *International Journal of Precision Engineering and Manufacturing-Green Technology, 9*(2), 431–441.
119. Lin, Y. H., Wang, Y. J., & Reshetnyak, V. (2017). Liquid crystal lenses with tunable focal length. *Liquid Crystals Reviews, 5*(2), 111–143.
120. Sensale-Rodriguez, B., Yan, R., Kelly, M. M., Fang, T., Tahy, K., Hwang, W. S., Jena, D., Liu, L., Xing, H. G. (2012). Broadband graphene terahertz modulators enabled by intraband transitions. *Nature Communications*, *3*, 780.
121. Lou, Y., Shen, S., Wang, C., & Chen, L. (2013). Design and fabrication of tunable liquid crystal diffractive lens. *Optical Engineering, 52*(9), 091713.
122. Ark, S. U. P., Ark, B. O. P., Am, S. A. N., Un, S. U. Y., Ark, S. E. K. O. O. P., Un, S. E. M., Im, J. E. M. O. O. K. L., Eonghwa, Y., Yu, R., Ong, S. E. O. K. H. O. S., & Yung, K. I. K. K. (2017). Electrically tunable binary phase Fresnel lens based on a dielectric elastomer actuator. *Optics Express, 25*(20), 23801–23808.
123. Fogle, F., Cierny, O., Do Vale Pereira, P., Kammerer, W., Cahoy, K. (2020). Miniature optical steerable antenna for intersatellite communications liquid lens characterization. IEEE Aerospace Conference Proceedings.
124. Wick, D., Cowan, W., Bagwell, B., Spahn, O. (2006). *Lightweight active optics for space and near space*. Sandia National Lab. (SNL-NM), Albuquerque, NM (United States).
125. Nandi, A., Palit, S., Debnath, D., Chakrabarti, S. K., Kotoch, T. B., Sarkar, R., Yadav, V. K., Girish, V., Rao, A. R., & Bhattacharya, D. (2011). Instruments of RT-2 experiment onboard CORONAS-PHOTON and their test and evaluation III: Coded Aperture Mask and Fresnel Zone Plates in RT-2/CZT payload. *Experimental Astronomy, 29*(1), 55–84.
126. Mingareev, I., Berlich, R., Eichelkraut, T. J., Herfurth, H., Heinemann, S., & Richardson, M. C. (2011). Diffractive optical elements utilized for efficiency enhancement of photovoltaic modules. *Optics Express, 19*(12), 11397.
127. Garnett, E. C., Ehrler, B., Polman, A., & Alarcon-Llado, E. (2021). Photonics for photovoltaics: Advances and opportunities. *ACS Photonics, 8*(1), 61–70.
128. Schumann, M. F., Langenhorst, M., Smeets, M., Ding, K., Paetzold, U. W., & Wegener, M. (2017). All-angle invisibility cloaking of contact fingers on solar cells by refractive free-form surfaces. *Advanced Optical Materials, 5*(17), 1–7.
129. Neo, D. C. J., Ong, M. M. X., Lee, Y. Y., Teo, E. J., Ong, Q., Tanoto, H., Xu, J., Ong, K. S., & Suresh, V. (2022). Shaping and tuning lighting conditions in controlled environment agriculture: A review. *ACS Agricultural Science & Technology, 2*(1), 3–16.
130. Kang, S. G., & Shin, J. (2021). Laser beam oscillation welding of aluminum alloy using the spatially modulated beam by diffractive optical element (DOE). *Journal of Manufacturing Processes, 66*, 387–396.
131. Pinilla, S., Miri Rostami, S. R., Shevkunov, I., Katkovnik, V., & Egiazarian, K. (2022). Hybrid diffractive optics design via hardware-in-the-loop methodology for achromatic extended-depth-of-field imaging. *Optics Express, 30*(18), 32633.
132. Grulkowski, I., Manzanera, S., Cwiklinski, L., Sobczuk, F., Karnowski, K., & Artal, P. (2018). Swept source optical coherence tomography and tunable lens technology for comprehensive imaging and biometry of the whole eye. *Optica, 5*(1), 52–59.
133. Gould, T. J., Burke, D., Bewersdorf, J., & Booth, M. J. (2012). Adaptive optics enables 3D STED microscopy in aberrating specimens. *Optics Express, 20*(19), 20998–21009.
134. Bisoyi, H. K., & Li, Q. (2022). Liquid crystals: Versatile self-organized smart soft materials. *Chem Rev, 122*, 4887–4926.
135. Uchida, J., Soberats, B., Gupta, M., & Kato, T. (2022). Advanced functional liquid crystals. *Advanced Materials, 34*(23), 1–33.
136. Goossens, K., Lava, K., Bielawski, C. W., & Binnemans, K. (2016). Ionic Liquid crystals: Versatile materials. *Chemical Reviews, 116*(8), 4643–4807.
137. Ikeda, T. (2003). Photomodulation of liquid crystal orientations for photonic applications. *J. Mater. Chem., 13*, 2037–2057.
138. Assanto, G., Minzoni, A. A., Smyth, N. F., Worthy, A. L. (2010). Refraction of nonlinear beams by localized refractive index changes in nematic liquid crystals. *Physical Review A: Atomic, Molecular, and Optical Physics*, *82*(5), 1–8.
139. Khoo, I. C., Diaz, A., Liou, J., Stinger, M. V., Huang, J., & Ma, Y. (2010). Liquid crystals tunable optical metamaterials. *IEEE Journal of Selected Topics in Quantum Electronics, 16*(2), 410–417.
140. Ikeda, T., Yoneyama, S., Yamamoto, T., & Hasegawa, M. (2002). Refractive-index modulation by means of photosensitive liquid crystals. *Molecular Crystals and Liquid Crystals, 375*(1), 45–60.

141. Assanto, G., Smyth, N. F., & Xia, W. (2011). Modulation analysis of nonlinear beam refraction at an interface in liquid crystals. *Physical Review A: Atomic, Molecular, and Optical Physics, 84*(3), 1–7.
142. Zhang, G., Schreier, A., Wang, X., Matthews, W., Farmer, J., Faulkner, G., Elston, S. J., Morris, S. M., & O'Brien, D. (2023). Free-space optical communication link with liquid crystal beam-steering. *IEEE Photonics Technology Letters, 35*(22), 1199–1202.
143. Feng, F., White, I. H., & Wilkinson, T. D. (2013). Free space communications with beam steering a two-electrode tapered laser diode using liquid-crystal slm. *Journal of Lightwave Technology, 31*(12), 2001–2007.
144. Winker, B., Mahajan, M., & Hunwardsen, M. (2004). Liquid crystal beam directors for airborne free-space optical communications. *IEEE Aerospace Conference Proceedings, 3*, 1702–1708.
145. Lin, Y.-H., Mahajan, M., Taber, D., Wen, B., Winker, B. (2005). Compact 4 cm aperture transmissive liquid crystal optical phased array for free-space optical communications. *Free Laser Commun V, 5892*(August 2005), 58920C.
146. Kim, J., Oh, C., Escuti, M. J., Hosting, L., Serati, S. (2008). Wide-angle nonmechanical beam steering using thin liquid crystal polarization gratings. *Proc of SPIE Vol, 7093*, 709302.
147. Li, J., Wen, C. H., Gauza, S., Lu, R., & Wu, S. T. (2005). Refractive indices of liquid crystals for display applications. *IEEE/OSA Journal of Display Technology, 1*(1), 51.
148. Huang, Y., He, Z., & Wu, S.-T. (2017). Fast-response liquid crystal phase modulators for augmented reality displays. *Optics Express, 25*(26), 32757–32766.
149. Yin, K., Hsiang, E. L., Zou, J., Li, Y., Yang, Z., Yang, Q., Lai, P. C., Lin, C. L., Wu, S. T. (2022) Advanced liquid crystal devices for augmented reality and virtual reality displays: Principles and applications. *Light: Science & Applications*, *11*(1).
150. Liu, S., Li, Y., & Su, Y. (2020). Multiplane displays based on liquid crystals for AR applications. *Journal of the Society for Information Display, 28*(3), 224–240.
151. Ju, L., Geng, B., Horng, J., Girit, C., Martin, M., Hao, Z., Bechtel, H. A., Liang, X., Zettl, A., Shen, Y. R., & Wang, F. (2011). Graphene plasmonics for tunable terahertz metamaterials. *Nature Nanotechnology, 6*(10), 630–634.
152. Lee, H., Lim, C. H. J., Low, M. J., Tham, N., Murukeshan, V. M., & Kim, Y. J. (2017). Lasers in additive manufacturing: A review. *International Journal of Precision Engineering and Manufacturing-Green Technology, 4*(3), 307–322.
153. Sensale-Rodriguez, B., Rafique, S., Yan, R., Zhu, M., Protasenko, V., Jena, D., Liu, L., & Xing, H. G. (2013). Terahertz imaging employing graphene modulator arrays. *Optics Express, 21*(2), 2324.
154. Malevich, Y., Ergoktas, M. S., Bakan, G., Steiner, P., & Kocabas, C. (2020). Video-speed graphene modulator arrays for terahertz imaging applications. *ACS Photonics, 7*(9), 2374–2380.
155. Tamagnone, M., Capdevila, S., Lombardo, A., Wu, J., Centeno, A., Zurutuza, A., Ionescu, A. M., Ferrari, A. C., Mosig, J. R. (2018). Graphene reflectarray metasurface for terahertz beam steering and phase modulation. *arXiv preprint arXiv*,1806.02202.
156. Li, P., Liu, X., Cheng, Q., & Liang, Z. (2021). Long-term photovoltaic performance of thin-film solar cells with diffractive microlens arrays on glass substrates. *Results Phys., 21*, 103841.
157. Tumbelaka, B. Y., Hidayat, D., Taufik, M., Novita, D., Suhendi, N. (2017). Converting solar energy to electricity energy using diffractive and selective crystalline photonics. *2016 International Seminar on Intelligent Technology and Its Applications (ISITIA)*, 493–496.
158. Shanks, K., Senthilarasu, S., & Mallick, T. K. (2016). Optics for concentrating photovoltaics: Trends, limits and opportunities for materials and design. *Renewable and Sustainable Energy Reviews, 60*, 394–407.
159. Mayer, J., Gallinet, B., Offermans, T., & Ferrini, R. (2016). Diffractive nanostructures for enhanced light-harvesting in organic photovoltaic devices. *Optics Express, 24*(2), A358.
160. Barkhouse, D. A. R., Gunawan, O., Gokmen, T., Todorov, T. K., & Mitzi, D. B. (2015). Yield predictions for photovoltaic power plants: Empirical validation, recent advances and remaining uncertainties. *Progress in Photovoltaics: Research and Applications, 20*(1), 6–11.
161. Kim, G., Dominguez-Caballero, J. A., Lee, H., Friedman, D. J., & Menon, R. (2013). Increased photovoltaic power output via diffractive spectrum separation. *Physical Review Letters, 110*(12), 1–5.
162. Alsaigh, R. E., Bauer, R., & Lavery, M. P. J. (2020). Multi-element lenslet array for efficient solar collection at extreme angles of incidence. *Science and Reports, 10*(1), 1–9.
163. Langenhorst, M., Ritzer, D., Kotz, F., Risch, P., Dottermusch, S., Roslizar, A., Schmager, R., Richards, B. S., Rapp, B. E., & Paetzold, U. W. (2019). Liquid glass for photovoltaics: Multifunctional front cover glass for solar modules. *ACS Applied Materials & Interfaces, 11*(38), 35015–35022.
164. Schumann, M. F., Wiesendanger, S., Goldschmidt, J. C., Bläsi, B., Bittkau, K., Paetzold, U. W., Sprafke, A., Wehrspohn, R. B., Rockstuhl, C., & Wegener, M. (2015). Cloaked contact grids on solar cells by coordinate transformations: Designs and prototypes. *Optica, 2*(10), 850–853.
165. Albarazanchi, A., Gérard, P., Ambs, P., Meyrueis, P., Nguyen, G.-N., & Heggarty, K. (2016). Smart multifunction diffractive lens experimental validation for future PV cell applications. *Optics Express, 24*(2), A139.
166. Tittl, A. (2022). Tunable structural colors on display. *Light Sci. Appl., 11*(1), 10–11.
167. Ke, Y., Chen, J., Lin, G., Wang, S., Zhou, Y., Yin, J., Lee, P. S., & Long, Y. (2019). Smart windows: Electro-, Thermo-, Mechano-, Photochromics, and Beyond. *Advanced Energy Materials, 9*(39), 1–38.
168. Huh, J.-W., Choi, T.-H., Woo, J.-H., Kim, J.-H., Do, S.-M., Seo, J.-H., Yoon, T.-H. (2020) Bistable liquid-crystal phase grating device for smart window and window display applications.,*Proc. of SPIE, 11303,* 113030J.
169. Han, C. H., Eo, H., Choi, T. H., Kim, W. S., & Oh, S. W. (2022). A simulation of diffractive liquid crystal smart window for privacy application. *Science and Reports, 12*(1), 1–12.
170. Chowdhary, A. K., Sikdar, D. (2021). Solar energy materials and solar cells design of electrotunable all-weather smart windows. *Solar Energy Materials & Solar Cells*, *222*, 110921.
171. Wang, S., Jiang, T., Meng, Y., Yang, R., Tan, G., Long, Y. (2021). Scalable thermochromic smart windows with passive radiative cooling regulation. *Science, 374*(6574), 1501–1504.
172. Perennes, F., Twardowski, P. J., Gesbert, D., Meyrueis, P. (1992). Phase-diffractive coating for daylight control on smart window. *Opt. Mater. Technol. Energy Effic. Sol. Energy Convers. XI Sel. Mater. Conc. Reflectors, Transparent Insul. Superwindows*, *1727*(November 1992), 368–374.
173. Pattison, P. M., Tsao, J. Y., Brainard, G. C., & Bugbee, B. (2018). LEDs for photons, physiology and food. *Nature, 563*(7732), 493–500.
174. Yeh, N., & Chung, J. P. (2009). High-brightness LEDs-Energy efficient lighting sources and their potential in indoor plant cultivation. *Renewable and Sustainable Energy Reviews, 13*(8), 2175–2180.
175. van Iersel, M. W., & Gianino, D. (2017). An adaptive control approach for light-emitting diode lights can reduce the energy costs of supplemental lighting in greenhouses. *HortScience, 52*(1), 72–77.

176. Tang, Y., Jia, M., Mei, Y., Yu, Y., Zhang, J., Tang, R., & Song, K. (2019). 3D intelligent supplement light illumination using hybrid sunlight and LED for greenhouse plants. *Optik, 183*, 367–374.
177. Parrish, C. H., Hebert, D., Jackson, A., Ramasamy, K., McDaniel, H., Giacomelli, G. A., & Bergren, M. R. (2021). Optimizing spectral quality with quantum dots to enhance crop yield in controlled environments. *Communications Biology, 4*(1), 1–9.
178. Benatar, A. (2007). Diffractive optics as beam-shaping elements for plastics laser welding. *Optical Engineering, 46*(11), 118001.
179. Kononenko, V. V., Konov, V. I., Pimenov, S. M., Prokhorov, A. M., Pavelyev, V. S., Soifer, V. A., Luedge, B., Duparre, M. R. (2002). Laser shaping of diamond for IR diffractive optical elements. *Second International Symposium on Laser Precision Microfabrication*, *4426*(February 2002), 128.
180. McDonnell, C., Coyne, E., & O'Connor, G. M. (2018). Greyscale silicon diffractive optics for selective laser ablation of thin conductive films. *Applied Optics, 57*(24), 6966–6970.
181. Račiukaitis, G., Stankevičius, E., Gečys, P., Gedvilas, M., Bischoff, C., Jäger, E., Umhofer, U., & Völklein, F. (2011). Laser processing by using diffractive optical laser beam shaping technique. *Journal of Laser Micro/Nanoengineering, 6*(1), 37–43.
182. Hammond, J. B., Johnson, E. G., Koehler, C. S., Stack, J. D., Suleski, T. J., Kar, A., Guo, W. (1999). Diffractive optics for laser welding and bonding. Diffractive Hologr. Technol. Syst. Spat. Light Modul. VI, *3633*(June 1999), 206–213.
183. Torres-Peiró, S., González-Ausejo, J., Mendoza-Yero, O., Mínguez-Vega, G., Andrés, P., & Lancis, J. (2013). Parallel laser micromachining based on diffractive optical elements with dispersion compensated femtosecond pulses. *Optics Express, 21*(26), 31830.
184. Katz, S., Kaplan, N., & Grossinger, I. (2018). Using diffractive optical elements: DOEs for beam shaping-fundamentals and applications. *Laser Technik Journal, 15*(4), 29–32.
185. Klein-Wiele, J. H., Blumenstein, A., Simon, P., & Ihlemann, J. (2020). Laser interference ablation by ultrashort UV laser pulses via diffractive beam management. *Advanced Optical Technologies, 9*, 41–52.
186. Clement, C. E., Thio, S. K., & Park, S. Y. (2017). An optofluidic tunable Fresnel lens for spatial focal control based on electrowetting-on-dielectric (EWOD). *Sensors Actuators, B Chem., 240*, 909–915.
187. Cheng, Y., Cao, J., Hao, Q. (2021). Optical beam steering using liquid-based devices. *Optics and Lasers in Engineering*, *146*(June 2020), 106700.
188. Schaal, F., Haist, T., Peter, A., Beeck, A., Pruss, C., Osten, W. (2014). Applications of diffractive optical elements for optical measurement techniques. *Hologr Diffractive Opt Appl VI*, *9271*(November 2014), 927105.
189. Hu, Y., Cui, Q., Zhao, L., & Piao, M. (2018). PSF model for diffractive optical elements with improved imaging performance in dual-waveband infrared systems. *Optics Express, 26*(21), 26845.
190. Wang, H., Liu, Y., Ruan, Q., Liu, H., Ng, R. J. H., Tan, Y. S., Wang, H., Li, Y., Qiu, C. W., & Yang, J. K. W. (2019). Off-axis holography with uniform illumination via 3D printed diffractive optical elements. *Advanced Optical Materials, 7*(12), 1–9.
191. Xie, X., Yu, X., Gao, X., Pei, X., Wang, Y., Sang, X., Yan, B. (2022). Extended depth of field method with a designed diffraction optical element based on multi-depth fusion and end-to-end optimization. *Optics Communication*, *517*(January), 128317.
192. Kern, C., Speck, U., Riesenberg, R., Reble, C., Khazaka, G., Zieger, M., Kaatz, M., De Gregorio, M., & Fischer, F. (2021). Mobile snapshot hyperspectral imaging device for skin evaluation using diffractive optical elements. *Skin Research and Technology, 27*(4), 589–598.
193. Xiong, Z., Kunwar, P., & Soman, P. (2021). Hydrogel-Based Diffractive Optical Elements (hDOEs) using rapid digital photopatterning. *Advanced Optical Materials., 9*(2), 1–11.
194. Lee, J., Lee, J., Du, X., Du, X., Park, J., Cui, Q., Iyer, R. R., Iyer, R. R., Boppart, S. A., Boppart, S. A., Boppart, S. A., & Gao, L. (2023). Tunable image-mapping optical coherence tomography. *Biomedical Optics Express, 14*(2), 627–638.
195. Booth, M., Andrade, D., Burke, D., Patton, B., & Zurauskas, M. (2015). Aberrations and adaptive optics in super-resolution microscopy. *Microscopy, 64*(4), 251–261.
196. Kim, C.-S., Kim, W., Lee, K., & Yoo, H. (2019). High-speed color three-dimensional measurement based on parallel confocal detection with a focus tunable lens. *Optics Express, 27*(20), 28466–28479.
197. Yun, S. H., Tearney, G. J., Vakoc, B. J., Shishkov, M., Oh, W. Y., Desjardins, A. E., Suter, M. J., Chan, R. C., Evans, J. A., Jang, I. K., Nishioka, N. S., De Boer, J. F., & Bouma, B. E. (2006). Comprehensive volumetric optical microscopy in vivo. *Nature Medicine, 12*(12), 1429–1433.
198. Kim, J., Xing, J., Nam, H. S., Song, J. W., Kim, J. W., & Yoo, H. (2017). Endoscopic micro-optical coherence tomography with extended depth of focus using a binary phase spatial filter. *Optics Letters, 42*(3), 379–382.
199. Pawlowski, M. E., Shrestha, S., Park, J., Applegate, B. E., Oghalai, J. S., & Tkaczyk, T. S. (2015). Miniature, minimally invasive, tunable endoscope for investigation of the middle ear. *Biomedical Optics Express, 6*(6), 2246–2257.
200. Zou, Y., Chau, F. S., & Zhou, G. (2017). Ultra-compact optical zoom endoscope using solid tunable lenses. *Optics Express, 25*(17), 20675–20688.
201. Aljasem, K., Froehly, L., Seifert, A., & Zappe, H. (2011). Scanning and tunable micro-optics for endoscopic optical coherence tomography. *J. Microelectromechanical Syst., 20*(6), 1462–1472.
202. Chong, C., Isamoto, K., & Toshiyoshi, H. (2006). Optically modulated MEMS scanning endoscope. *IEEE Photonics Technology Letters, 18*(1), 133–135.
203. Zhen, Q., & Piyawattanamatha, W. (2017). New endoscopic imaging technology based on MEMS sensors and actuators. *Micromachines, 8*(7), 210.
204. Piyawattanametha, W., Ra, H., Loewke, K. E., Mandella, M. J., Contag, C. H., Qiu, Z., Wang, T. D., Friedland, S., Liu, J. T., Kino, G. S., & Solgaard, O. (2012). In vivo near-infrared dual-axis confocal microendoscopy in the human lower gastrointestinal tract. *Journal of Biomedial Optics, 17*(02), 021102–021102.
205. El-kady, M. F., Kaner, R. B., Angeles, L., States, U., Science, M., Angeles, L., States, U. (2014). Direct laser writing of graphene. *9*, 8725–8729.
206. Li, G. (2020). Direct laser writing of graphene electrodes. *J Appl Phys, 127*, 010901
207. Zuo, P., Jiang, L., Li, X., Tian, M., Xu, C., Yuan, Y., Ran, P., & Li, B. (2019). Maskless Micro/Nanopatterning and bipolar electrical recti fi cation of MoS 2 flakes through femtosecond laser direct writing. *ACS Appl Mater Interfaces, 11*(42), 39334–39341.
208. Tang, J., Yi, W., Zhong, X., John, C., Xiao, X., Pan, F., & Xu, B. (2020). Laser writing of the restacked titanium carbide MXene for high performance supercapacitors. *Energy Storage Materials, 32*, 418–424.
209. Tian, Q., Yin, P., Zhang, T., Zhou, L., Xu, B., Luo, Z., & Liu, H. (2020). MXene $Ti_3C_2T_x$ saturable absorber for passively Q-switched mid-infrared laser operation of femtosecond-laser–inscribed Er:Y_2O_3ceramic channel waveguide abrication and characterization. *Nanophotonics, 9*(8), 2495–2503.

Publisher's Note Springer Nature remains neutral with regard to jurisdictional claims in published maps and institutional affiliations.

Dongwook Yang received his BS and MS degree in Department of Mechanical Engineering from Korea Advanced Institute of Science and Technology (KAIST). He is a currently Phd Candidate in Department of Mechanical Engineering from Korea Advanced Institute of Science and Technology (KAIST). His research interest is femtosecond laser processing, direct laser writing of flexible/stretchable electronics/energy storage, and laser-induced graphene (LIG).

Guseon Kang received his BS and MS degree in Department of Mechanical Engineering from Korea Advanced Institute of Science and Technology (KAIST) in 2015 and 2017, respectively. He was a researcher at the Korea Institute of Industrial Technology (KITECH) until July 2021. He is currently a Ph.D. candidate in Department of Mechanical Engineering at KAIST. His current research interest is high-precision optical and terahertz metrology using the optical frequency comb.

Younggeun Lee received his BS and MS degrees in the Department of Mechanical Engineering from Hanyang University. He is currently a PhD candidate in the Department of Mechanical Engineering at the Korea Advanced Institute of Science and Technology (KAIST). His research interests include femtosecond laser processing and direct laser writing of optics with laser-induced graphene (LIG).

Seung Eon Lee earned his BS and MS degrees in the Department of Mechanical Engineering from Korea Advanced Institute of Science and Technology (KAIST) in 2021 and 2023 respectively. He is currently a PhD candidate at KAIST. His research interests include optical imaging modalities, such as optical coherence tomography and confocal microscopy.

Hyeokin Kang received his BS and MS degree in Department of Mechanical System Design Engineering from Seoul National University of Science and Technology (SEOULTECH). He is a currently Phd Candidate in Department of Mechanical Engineering from Korea Advanced Institute of Science and Technology (KAIST). His research interest is free-space optical communication based on femtosecond laser, design and performance evaluation of diffractive optical elements.

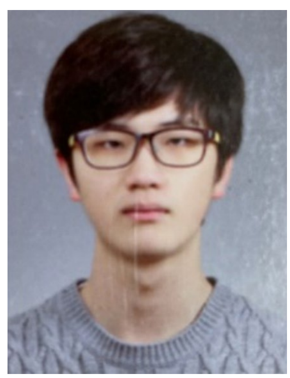

Hyogeun Han received his BS and MS degree in the Department of Aerospace Engineering at Korea Advanced Institute of Science and Technology (KAIST). He is currently a Ph.D candidate student in the Department of Aerospace Engineering at KAIST. His academic research focuses on Orbit Determination and Navigation, and spacecraft's Attitude Sensor, such as Star Tracker and Sun Sensor.

Quang Huy Vu received his MS and Ph.D. degrees in the Department of Mechanical System Design Engineering, at Seoul National University of Science and Technology (SEOULTECH). He is a senior researcher at the Institute of Precision Machinery Technology (SEOULTECH). His research interests are optical metrology, diffractive optical elements, lens design, hyperspectral imaging, imaging system and system calibration.

Seunghwan Kim is a master's student in the Department of Aerospace Engineering at the Korea Advanced Institute of Science and Technology (KAIST). His academic research focuses on developing sun sensors, including image processing and hardware design, as well as Global Navigation Satellite System (GNSS) receivers for atmospheric monitoring.

Han Ku Nam is a postdoctoral researcher in Department of Mechanical Engineering in KAIST, Korea. He received his Ph.D. degree from KAIST in 2023, and he received his MS degree in Department of Mechanical Engineering from State University of New York (SUNY) at Stony Brook in 2018. He received his BS degrees in Department of Mechanical Engineering from SUNY at Stony Brook and Ajou University in 2017 and 2018 respectively through dual-degree program. His research interests include ultrafast material processing, direct laser writing of flexible/stretchable electronics, lignocellulosic materials, and laser-induced graphene (LIG).

Soongeun Kwon is a principal researcher of Nano Lithography & Manufacturing Research Center at Korea Institute of Machinery and Materials (KIMM). He is also an adjunct professor in the Department of Mechanical Engineering in University of Science & Technology (UST). He received his B.S., M.S., and Ph.D. degrees in mechanical engineering at Korea Advanced Institute of Science and Technology (KAIST), respectively. His research interest is on the development of nano/micro patterning process and application of energy storage devices based on carbon nanomaterials.

Hyug-Gyo Rhee received the Ph.D. degree in Department of Mechanical Engineering from Korea Advanced Institute of Science and Technology, Daejeon, South Korea, in 2003. He was with the National Institute of Standard and Technology, USA, as a Guest Researcher from 2003 to 2005. He is currently with the Korea Research Institute of Standards and Science, Daejeon, with research area of high-resolution imaging system, adaptive optics, freeform optics, and direct laser lithography.

Joohyung Lee is an Associate professor in the Department of Mechanical System Design Engineering, at Seoul National University of Science and Technology University (SEOULTECH). He received his Ph.D. degree from Korea Advanced Institute of Science and Technology (KAIST). His research interests are optical frequency comb, precision metrology, and optical design.

Hongki Yoo received his BS, MS, and PhD degrees in Mechanical Engineering from Korea Advanced Institute of Science and Technology (KAIST) in 2001, 2003, and 2007 respectively. Before joining the KAIST in 2019, he worked in the field of biomedical optics in Wellman Center for Photomedicine at Harvard Medical School and Massachusetts General Hospital, as well as in Hanyang University. He is currently an associate professor of Mechanical Engineering at KAIST. His research focuses on developing novel optical methods including confocal microscopy, optical coherence tomography, fluorescence molecular imaging, and endoscopic probes to solve challenging medical problems and address industrial metrology needs.

Hyosang Yoon received his BS and MS degrees in the Department of Aerospace Engineering at the Korea Advanced Institute of Science and Technology (KAIST) in 2008 and 2010, respectively. He received his Ph.D degree in the Department of Aeronautics and Astronautics at Massachusetts Institute of Technology (MIT) in 2017. He worked as an engineer at Satrec Initiative from 2008 to 2014, and Planet Labs from 2017 to 2019. He is currently an assistant professor in the Department of Aerospace and Engineering in KAIST from 2019. His research focuses on Laser communication of CubeSats, Inter-satellite Optical Communication System, the Development of Technologies for LEO Satellites, and GNSS Radio Occultation (RO) Software Defined Radio (SDR) for CubeSats.

Young Jin Kim earned his BS, MS, and PhD degrees in Department of Mechanical Engineering from Korea Advanced Institute of Science and Technology (KAIST) in 2002, 2004, and 2008 respectively. He was an assistant professor in School of Mechanical and Aerospace Engineering of Nanyang Technological University (NTU) from 2014 to 2019. He is a currently associate professor in Department of Mechanical Engineering of KAIST from 2019. His research interest is on ultrafast photonics and its applications in high-precision metrology, surface topography, biomedical diagnosis, space LIDARs and nano/micro material processing.